nature

https://doi.org/10.1038/s41586-023-06750-w

Accelerated Article Preview

Antigenicity and receptor affinity of SARS-CoV-2 BA.2.86 spike

Received: 11 September 2023

Accepted: 16 October 2023

Accelerated Article Preview

Cite this article as: Wang, Q. et al. Antigenicity and receptor affinity of SARS-CoV-2 BA.2.86 spike. *Nature* https://doi.org/10.1038/s41586-023-06750-w (2023)

Qian Wang, Yicheng Guo, Liyuan Liu, Logan T. Schwanz, Zhiteng Li, Manoj S. Nair, Jerren Ho, Richard M. Zhang, Sho Iketani, Jian Yu, Yiming Huang, Yiming Qu, Riccardo Valdez, Adam S. Lauring, Yaoxing Huang, Aubree Gordon, Harris H. Wang, Lihong Liu & David D. Ho

Antigenicity and receptor affinity of SARS-CoV-2 BA.2.86 spike

Qian Wang[1*], Yicheng Guo[1*], Liyuan Liu[2*], Logan T. Schwanz[2,3], Zhiteng Li[1], Manoj S. Nair[1], Jerren Ho[1], Richard M. Zhang[1], Sho Iketani[1], Jian Yu[1], Yiming Huang[2], Yiming Qu[2], Riccardo Valdez[4], Adam S. Lauring[5,6], Yaoxing Huang[1,7], Aubree Gordon[4], Harris H. Wang[2], Lihong Liu[1,7#], and David D. Ho[1,7,8#]

[1]Aaron Diamond AIDS Research Center, Columbia University Vagelos College of Physicians and Surgeons, New York, NY, USA.

[2]Department of Systems Biology, Columbia University Vagelos College of Physicians and Surgeons, New York, NY, USA.

[3]Department of Pathobiology and Mechanisms of Disease, Columbia University Irving Medical Center, New York, NY, USA.

[4]Department of Pathology, University of Michigan, Ann Arbor, MI, USA.

[5]Department of Internal Medicine, University of Michigan, Ann Arbor, MI, USA.

[6]Department of Microbiology and Immunology, University of Michigan, Ann Arbor, MI, USA.

[7]Department of Medicine, Columbia University Vagelos College of Physicians and Surgeons, New York, NY, USA.

[8]Department of Microbiology and Immunology, Columbia University Vagelos College of Physicians and Surgeons, New York, NY, USA.

[*]Equal contribution

[#]Correspondence: Lihong Liu (ll3411@cumc.columbia.edu), David D. Ho (dh2994@cumc.columbia.edu)

Abstract

A SARS-CoV-2 Omicron subvariant, BA.2.86, has emerged and spread to numerous countries worldwide, raising alarm because its spike protein contains 34 additional mutations compared to its BA.2 predecessor[1]. We examined its antigenicity using human sera and monoclonal antibodies (mAbs). Reassuringly, BA.2.86 was not more resistant to human sera than the currently dominant XBB.1.5 and EG.5.1, indicating that the new subvariant would not have a growth advantage in this regard. Importantly, sera from patients who had XBB breakthrough infection exhibited robust neutralizing activity against all viruses tested, suggesting that upcoming XBB.1.5 monovalent vaccines could confer added protection. While BA.2.86 showed greater resistance to mAbs to subdomain 1 (SD1) and receptor-binding domain (RBD) class 2 and 3 epitopes, it was more sensitive to mAbs to class 1 and 4/1 epitopes in the "inner face" of RBD that is exposed only when this domain is in the "up" position. We also identified six new spike mutations that mediate antibody resistance, including E554K that threatens SD1 mAbs in clinical development. The BA.2.86 spike also had a remarkably high receptor affinity. The ultimate trajectory of this new SARS-CoV-2 variant will soon be revealed by continuing surveillance, but its worldwide spread is worrisome.

Key words: COVID-19, SARS-CoV-2, XBB.1.5, EG.5.1, BA.2.86, polyclonal sera; monoclonal antibodies, mRNA vaccines, antibody evasion, receptor binding affinity

INTRODUCTION

Although the COVID-19 pandemic has officially ended[2], SARS-CoV-2 continues to spread and evolve. Recent infections have been dominated by XBB.1.5 and EG.5.1 subvariants[3]. A highly mutated SARS-CoV-2 Omicron subvariant, designated BA.2.86, was first reported only recently, and it is genetically distinct from the prevailing viruses in the XBB sublineage[3-6]. The genetic distance to its predecessor, BA.2, is equivalent to that between BA.1 and the Delta variant (**Figure 1a**), raising the same antibody evasion concerns when the first Omicron variant emerged in late 2021. Over 430 sequences of BA.2.86 has been found in 28 countries[1] already despite limited surveillance nowadays. A recent outbreak due to the new subvariant in a nursing facility in England with high attack rate among residents and staff shows BA.2.86 is readily transmissible[7]. At present, there is little clinical evidence to address its pathogenicity.

Compared with the spike of BA.2, BA.2.86 possesses 34 additional mutations, including 13 mutations in the N-terminal domain (NTD), 14 in RBD, 2 in SD1, 3 in the subdomain 2 (SD2), and 2 in the S2 region (**Figures 1b and 1c**). Mutations H69V70 deletion (H69V70Δ), Y144 deletion (Y144Δ), G446S, N460K, F486P, and R493Q have been identified previously[5,6,8,9], but mutations V445H, N450D, N481K, V483 deletion (V483Δ), and E554K have been seldom observed in circulating viruses (**Figure 1c**). This extensive array of spike mutations in BA.2.86 is alarming because of the heightened potential for the virus to evade serum antibodies elicited by prior infections and/or vaccinations or mAbs intended for clinical use. The present study addresses this concern by characterizing the antigenicity of BA.2.86 spike using multiple collections of human sera and a large panel of mAbs.

RESULTS

Sequence variation

The initial analysis of available BA.2.86 spike sequences was challenging due to sequence variations and uncertainties. A four amino-acid insertion after the V16 residue (V16insMPLF) was observed in a majority of reported sequences, while some were ambiguous because of low sequencing quality spanning this region (**Extended Data Figure 1**). We therefore made the determination that V16insMPLF should be included in our spike construct. Another variation is the presence or absence of the I670V mutation. Before it was recognized that most BA.2.86 strains do not contain this mutation (**Extended Data Figure 1**), we already synthesized both spike genes by methods previously described[4,10]: BA.2.86-V1 being the dominant form and BA.2.86-V2 being the minor form (**Figure 1c**).

Serum neutralization

To assess the antigenicity of the BA.2.86 spike, we constructed vesicular stomatitis virus (VSV) pseudotyped viruses using both versions of the spike gene, as well as BA.2, XBB.1.5, and EG.5.1 pseudoviruses for comparison. These pseudoviruses were then subjected to neutralization studies using serum samples from three distinct clinical cohorts. The first cohort consisted of healthy individuals who received three doses of monovalent mRNA vaccines followed by two doses of BA.5 bivalent mRNA vaccines (referred to as "3 shots monovalent + 2 shots bivalent"). The other two cohorts included patients who experienced a breakthrough infection caused by BA.2 (labeled as "BA.2 breakthrough") or XBB (labeled as "XBB breakthrough") after multiple vaccinations. More details on the clinical samples can be found in **Extended Data Table 1**.

The serum neutralization results and comparative analyses are shown in **Figure 2a** and **Figure 2b**, respectively. BA.2.86-V1 and BA.2.86-V2 displayed comparable neutralization ID_{50} (50% inhibitory dilution) titers across all three cohorts, indicating that the I670V mutation has no appreciable antigenic impact. Among the variants tested, BA.2 was most sensitive to neutralization by sera from all three cohorts. Surprisingly, BA.2.86 was not the most resistant; EG.5.1 was instead. In fact, compared to XBB.1.5 and EG.5.1, BA.2.86 was 1.5- and 2.0-fold, respectively, more sensitive to neutralization by sera from the "3 shots monovalent + 2 shots bivalent" cohort. BA.2.86 was also more sensitive to neutralization by sera from the "BA.2 breakthrough" cohort than EG.5.1 by 1.9-fold. BA.2.86, XBB.1.5, and EG.5.1 were similarly sensitive to neutralization by sera from the "XBB breakthrough" cohort; notably, the serum ID_{50} titers were quite robust, ranging from 729 to 879. This important observation was qualitatively confirmed using the same serum samples to neutralize EG.5.1 and BA.2.86 authentic viruses (**Extended Data Figure 2**). These results suggest that exposure to the spike of XBB.1.5 could lead to an effective antibody response against the current circulating SARS-CoV-2 variants, an inference that bodes well for the upcoming XBB.1.5 monovalent vaccines.

The serum neutralization data were then used to generate antigenic maps to graphically show the antigenic relationships between BA.2.86 and the other Omicron subvariants tested (**Figure 2c**). The scientific conclusions are obviously the same as those already stated, but such a display allows easier visualization of the overall findings.

Neutralization by mAbs

To understand the antibody evasion properties of BA.2.86 in greater detail, we evaluated the susceptibility of the dominant form, BA.2.86-V1, to neutralization by a panel of 26 mAbs that retained activity against BA.2. XBB.1.5 and EG.5.1 were included as comparators. Among the mAbs, 20 target the four epitope classes in the RBD[11], including S2K146[ref.12], BD57-0129[ref.13], BD56-1302[ref.13], DB56-1854[ref.13], Omi-3[ref.14], Omi-18[ref.14], BD-515[ref.15], Omi-42[ref.14], COV2-2196 (tixagevimab)[16], XGv347[ref.17], ZCB11[ref.18], XGv051[ref.17], A19-46.1[ref.19], S309 (sotrovimab)[20], COV2-2130 (cilgavimab)[16], LY-CoV1404 (bebtelovimab)[21], Beta-54[ref.22], BD55-4637[ref.13], SA55[ref.23], and 10-40[24]. The other 6 mAbs were C1520[ref.25] targeting the NTD, C1717[ref.25]

targeting both the NTD and subdomain 2 (NTD-SD2), and 4 SD1-directed monoclonals, including S3H3[ref.26], C68.59[ref.27], and two antibodies (ADARC1 and ADARC2) that we have been characterizing (our unpublished results). The raw IC_{50} (50% inhibitory concentration) values are shown in **Extended Data Table 2,** and fold changes in IC_{50} titers relative to BA.2 are summarized in **Figure 3a**.

Our results revealed that BA.2.86 was completely or substantially resistant to neutralization by mAbs to NTD, SD1, and RBD class 2 and class 3 epitopes, and the extent of its evasion from such antibodies appeared larger than those exhibited by XBB.1.5 and EG.5.1. In particular, BA.2.86 showed greater resistance to class 2 mAb XGv051 and class 3 mAbs S309 and Beta-54, while escaping almost completely from SD1 mAbs that could neutralize both XBB.1.5 and EG.5.1. Unexpectedly, BA.2.86 was substantially more sensitive to neutralization than EG.5.1 by a majority mAbs to class 1 and class 4/1 epitopes on the 'inner face' of RBD that are only revealed when this domain is in the "up" position[11,28]. This observation suggests that the RBD of BA.2.86 may be more exposed and accessible to certain antibodies. Overall, the opposing effects of different mutations on different classes of antibodies also explain, in part, why the longer genetic distance did not translate into a larger antigenic distance for BA.2.86.

To elucidate the impact of each BA.2.86 spike mutations on its antigenicity, we synthesized the gene for each of the 34 point mutants in the background of BA.2 and then constructed the corresponding pseudoviruses for neutralization studies using the same panel of mAbs (**Figure 3a**). The H245N mutation mediated resistance to the NTD antibody C1520. Significantly, the E554K mutation conferred evasion to all SD1-directed antibodies tested, which is in line with the report on C68.59 [ref.27]. Structural modeling suggests that E554K removes the salt bridge formed between E554 and R96 in the CDRL3 region of mAb S3H3 and induces steric hindrance that disrupts antibody binding (**Figure 3b**). Mutations N460K and F486P, also shared by XBB.1.5 and EG.5.1, mediated resistance to some RBD class 1 and/or class 2 mAbs. Specifically, the N460K mutation, first observed in the BA.2.75 variant, disrupts a key hydrogen bond between the RBD and VH3-53-encoded class 1 antibodies[29], while enhancing receptor affinity[30] at the same time. The F486P mutation appears to reduce the hydrophobic interaction with the ACE2-mimicking antibody S2K146 (**Figure 3c)**, hence impairing its neutralization activity. The K356T mutation, also shared by the DS.1 variant, conferred broad resistance to a number of RBD class 1, class 2, and class 3 mAb, possibly due to steric hindrance caused by the introduction of an additional glycosylation site[8]. Several other RBD mutations, including V445H, N450D, L452W, and A484K compromised the neutralizing activity of some RBD class 3 mAbs. Structural modeling indicates that N450D could form an additional salt bridge with R346, thereby altering the local conformation and resulting in resistance to mAbs such as COV2-2130 (**Figure 3d)**. On the other hand, mutations V445H and L452W seem to introduce steric clashes with the CDRs of RBD class 3 mAbs LY-CoV1404 (**Figure 3e**) and A19-46.1 (**Figure 3f**), respectively. Importantly, we also found two new mutations (S50L and I332V) that conferred a degree of sensitization to neutralization by certain mAbs, along with two previously known mutations (R403K and R493Q)

that were also sensitizing[8,9,31] (**Figure 3a**). The antibody sensitization effects of these four mutations were confirmed by studies on their reverse mutations. Each BA.2.86 pseudovirus carrying the individual "back mutation" generally became more resistant to RBD class 1 and 4/1 mAbs relative to the unmodified BA.2.86 (**Figure 3g and Extended Data Table 3**). The rest of the new mutations that are unique to BA.2.86 showed only minor or no effect on its antigenicity as assessed by this panel of mAbs. In summary, a number of mutations in this new variant caused resistance to antibody neutralization, and several other mutations mediated an opposite effect, while the remainder were antigenically neutral.

Receptor affinity

We also expanded our studies on the BA.2.86 spike by measuring its binding affinity to the viral receptor. The spike proteins of BA.2.86-V1 and BA.2.86-V2, along with those of BA.2, XBB.1.5, and EG.5.1 were first examined for binding to a dimeric human-ACE2-Fc protein by surface plasmon resonance (SPR) as we have previously reported[9]. XBB.1.5 and EG.5.1 spikes exhibited comparable affinities to ACE2, with K_D values of 1.34 nM and 1.21 nM, respectively (**Figure 4a**). These values represent only a modest increase in receptor binding affinity compared to the K_D value of the BA.2 spike (1.68 nM). In contrast, both versions of the BA.2.86 spikes showed a >2-fold increase in binding affinity, with similar K_D values of 0.54 nM and 0.60 nM, largely due to lower dissociation rates (K_d).

To corroborate these findings, we also evaluated the susceptibility of both BA.2.86 pseudoviruses to neutralization by the dimeric human-ACE2-Fc protein, in comparison to BA.2, XBB.1.5, and EG.5.1. In agreement with the SPR data, both versions of BA.2.86 were >2-fold more sensitive to ACE2 inhibition than XBB.1.5 and EG.5.1, as determined by their IC_{50} values (**Figure 4b**). A potential explanation for this heightened affinity may reside in the intrinsic charge properties of the two interacting molecules. The region of human ACE2 targeted by the RBD is negatively charged, while the Omicron RBD itself is positively charged[32]. The higher receptor binding affinity of the BA.2.86 spike might be attributed to the additional positive charges associated with mutations V445H, N460K, N481K and A484K (**Figure 4c**). Only the N460K mutation is shared with the spikes from XBB.1.5 and EG.5.1.

Discussion

SARS-CoV-2 variant BA.2.86 has raised alarm because of the extensive array of mutations in its spike protein. Current concerns about its antibody evasiveness are reminiscent of those when the first Omicron appeared in late 2021. We have therefore undertaken a thorough antigenic characterization of BA.2.86, and our findings have important clinical and scientific implications.

On the clinical front, our data showed that, compared to the currently dominant subvariants

XBB.1.5 and EG.5.1, BA.2.86 did not exhibit greater resistance to neutralization by human sera from three different cohorts in the United States (**Figure 2a**). In fact, it was slightly but appreciably more sensitive to serum neutralization than EG.5.1 (**Figure 2b**). Our results are in concordance with findings by Lasrado et al[33] from the US, observations by An et al[34] from China, and results by Khan et al[35] from South Africa, but in contrast with those posted by Yang et al from China[36], Uriu et al from Japan[37], and Sheward et al from Sweden[38], who found BA.2.86 to be slightly more resistant to antibodies in human sera than other XBB subvariants such as XBB.1.5 or EG.5.1. The discrepancy with the latter reports could be due to differences in the histories of exposures to SARS-CoV-2 infection and/or vaccination. Going forward, it will be important to understand the basis of the observed discrepancies, because relatively greater resistance to antibody neutralization could confer an advantage for the new variant to grow in the population.

Another clinical ramification of our findings is that the upcoming XBB.1.5 monovalent vaccines are likely to elicit an adequate antibody response to not only BA.2.86 but also the currently dominant subvariants XBB.1.5 and EG.5.1. This reassuring conclusion is inferred from our results showing that sera from the "XBB breakthrough" cohort exhibited robust neutralization titers against all viral variants tested (**Figure 2a and Extended Data Figure 2**), but more importantly it is now confirmed by results just posted by Moderna on its monovalent XBB.1.5 mRNA vaccine[39]. They too noted that BA.2.86 was not more resistant to antibody neutralization than XBB.1.5 and EG.5.1.

A third clinically relevant result is the loss of neutralizing activity for all of the SD1-directed mAbs we tested against BA.2.86. One previous study highlighted that SD1 antibodies are rarely induced by infection or vaccination[27], raising the specter that such antibodies could possibly maintain its neutralizing activity durably in the face of continuing SARS-CoV-2 evolution and become ideal candidates for clinical development. Regrettably, BA.2.86 by making the E554K mutation (**Figure 3a**) has dashed any such hope.

Our detailed studies on a panel of mAbs have also yielded important scientific insights on the evolutionary pathways taken by SARS-CoV-2. We have previously noted that Omicron subvariant XBC.1.6 exhibited a longer genetic distance from the ancestral virus than EG.5.1, and yet it was more sensitive to antibody neutralization than EG.5.1[ref.3]. That observation remained unexplained, but now a parallel situation has arisen with BA.2.86 that could be partially explained by our new findings. While BA.2.86 showed greater resistance to mAbs to SD1 and RBD class 2 and 3 epitopes, it was more sensitive to mAbs to RBD class 1 and 4/1 epitopes (**Figure 3a**). Moreover, a number of its mutations (e.g., K356T, V445H, N450D, E460K, F486P, and E554K) conferred antibody resistance, but their neutralizing effects are offset by other mutations (e.g., S50L, I332V, R403K, and R493Q) that conferred antibody sensitization.

Another scientific implication of our results is that the RBD of BA.2.86 is likely to be more exposed than the RBD of XBB.1.5 or EG.5.1. This conclusion is inferred from the above

observation that the new variant is more sensitive than XBB.1.5 or EG.5.1 to neutralization by class 1 and 4/1 mAbs, which target the "inner face" of RBD only when this domain is in the "up" position. Since receptor binding also occurs when the RBD is "up", this conclusion is in line with the finding that the spike of BA.2.86 has a >2-fold higher affinity for the viral receptor compared to the spike of XBB.1.5 or EG.5.1 (**Figures 4a and 4b**). In fact, BA.2.86 spike has one of the highest receptor affinities we have measured, together with the spikes of some of the viruses in the BA.2.75 sublineage[8] but the K_D is undoubtedly determined by additional properties including the electrostatic charge of the RBD (**Figures 4c**).

We have witnessed, almost in real time, the evolution of SARS-CoV-2 over the past three years. Studies on the successive waves of viral variants and subvariants have taught us that this virus is constantly mutating to evade pressure exerted by antibodies in human sera. Given the extent of herd immunity today, only the most antibody resistant forms will have a growth advantage and become dominant. At the same time, the spikes of recently dominant variants all possess high receptor affinity, which is one measure of viral fitness. The trajectory of BA.2.86 ahead will be determined by the characteristics described herein as well as by viral mutations beyond spike and yet to be defined host factors. However, the fact that this emerging variant has already spread to so many different countries scattered around the world would suggest that it must be quite fit, and that continuing surveillance is imperative.

Figures and legends

Figure 1. Divergence of BA.2.86 spike sequence from major SARS-CoV-2 variants.

a. Phylogenetic tree of SARS-CoV-2 variants based on spike sequences.
b. Location of mutations detected in BA.2.86 spike, relative to its ancestral BA.2 (PDB 7KRR[40]). The red, blue, cyan, orange, and green mutations are in RBD, NTD, SD1, SD2, and S2, respectively. The orange circle indicates the H681R mutation located proximal to the furin cleavage site. I670V denoted by an asterisk since it is found in only a minority of BA.2.86 spikes (BA.2.86-V2); the dominant form does not have this mutation (BA.2.86-V1). ins, insertion; Δ, deletion.
c. Spike mutations found in BA.2.86 and other SARS-CoV-2 variants compared with BA.2.

Figure 2. Serum neutralization of BA.2.86 compared with BA.2, XBB.1.5, and EG.5.1.

a. Neutralizing ID_{50} titers of serum samples from "3 shots monovalent + 2 shots bivalent", "BA.2 breakthrough" and "XBB breakthrough" cohorts against the indicated SARS-CoV-2 variants. The geometric mean ID_{50} titers (GMT) are presented above symbols. The neutralization assay limit of detection (dotted line) is 25. Statistical analyses were performed by employing Wilcoxon matched-pairs signed-rank tests. n, sample size. dpv, days post last vaccination; dpi, days post infection. BA.2.86-V2 carries an I670V mutation compared to the dominant version of BA.2.86 (BA.2.86-V1). The results shown are representative of those obtained in two independent experiments.
b. Fold changes in GMT relative to BA.2, XBB.1.5, and EG.5.1, with resistance colored red and sensitization colored green.
c. Antigenic map generated using neutralization data from panel A. BA.2 represents the central reference for all serum cohorts, with the antigenic distances calculated by the average divergence from each variant. One antigenic unit (AU) represents an approximately 2-fold change in ID_{50} titer.

Figure 3. Neutralization of BA.2.86 and its point mutants in BA.2 by a panel of mAbs.

a. Fold changes in IC_{50} values of XBB.1.5, EG.5.1, BA.2.86-V1, and point mutants relative to BA.2, with resistance colored red and sensitization colored green. "/", fold change not available as the IC_{50} value was below the limit of detection (< 0.001 μg/mL). The results shown are representative of those obtained in two independent experiments.
b-f. Structural modeling of how single mutations affect S3H3 [PDB 7WKA[26]] (b), S2K146 [PDB 7TAS[12]] (c), COV2-2130 [PDB 8D8Q[41]] (d), LY-CoV1404 [PDB 7MMO[21]] (e), and A19-46.1 [PDB 7TCA[42]] (f) neutralization. Dashed lines indicate salt bridges or hydrogen bonds. Red plates indicate steric hindrance. The surfaces are colored according to the electrostatic potential of mAb S2K146.
g. Fold changes in IC_{50} values of BA.2.86-V1 carrying back mutations L50S, V332I, K403R, and Q493R, relative to BA.2, with resistance colored red and sensitization colored green.

Figure 4. BA.2.86 exhibited stronger receptor affinity than BA.2, XBB.1.5 and EG.5.1.

a. ACE2 receptor binding affinity of BA.2.86 spike, in comparison with spikes from BA.2, XBB.1.5, and EG.5.1 as tested by SPR. Data shown are representative of those obtained in two independent experiments.

b. Susceptibility of two versions of BA.2.86 pseudoviruses to hACE2 inhibition, relative to that of BA.2, XBB.1.5, and EG.5.1. Data are representative of those obtained in two independent experiments and shown as mean ± standard error of mean (SEM) from triplicate measurements.

c. Electrostatic potential of hACE2 and the BA.2 RBD (PDB 7ZF7[14]), with arrows indicating the mutations identified in BA.2.86. The green and cyan boundaries delineate the footprints of the RBD and hACE2, respectively. The dashed lines showed the corresponding interaction surfaces between RBD and hACE2. Residues with positive and negative charges are colored as blue and red, respectively.

ACKNOWLEDGEMENTS

This study was supported by funding from the NIH SARS-CoV-2 Assessment of Viral Evolution (SAVE) Program and through the National Institutes of Health Collaborative Influenza Vaccine Innovation Center (75N93021C00014) attributed to D.D.H. and the NIH, NIAID under contract number 75N93019C00051 attributed to A.G. We acknowledge funding support from the NSF (MCB-2032259) attributed to H.H.W. We thank all who contributed their data to GISAID. We express our gratitude to David Manthei, Carmen Gherasim, Victoria Blanc, Pamela Bennett-Baker, Savanna Sneeringer, Lauren Warsinske, Theresa Kowalski-Dobson, Alyssa Meyers, Zijin Chu, Hailey Kuiken, Lonnie Barnes, Ashley Eckard, Kathleen Lindsey, Dawson Davis, Aaron Rico, Gabriel Simjanovski, Mayurika Patel, and Nivea Vydiswaran of the IASO study team for supplying serum samples. We acknowledge Michael T. Yin and Magdalena E. Sobieszczyk at Columbia University Medical Center for providing serum samples.

AUTHOR CONTRIBUTIONS

Lihong L. and D.D.H. conceived and supervised this project. Q.W. managed the project. Liyuan L., L.T.S., Y.H., Y.Q., and H.H.W. constructed the spike expression plasmids. Q.W., J.H., R.M.Z., and Lihong L. conducted pseudovirus neutralization assays. M.S.N. and Y.H. conducted authentic virus neutralization assays. Q.W. and Lihong L. purified SARS-CoV-2 soluble spike proteins and hACE2 protein. Y.G. conducted bioinformatic analyses. Q.W., Lihong L., J.H., S.I., and J.Y. purified antibodies. Z.L. performed SPR assay. R.V., A.S.L., and A.G. provided clinical samples. Q.W., Y.G., Lihong L., and D.D.H. analyzed the results and wrote the manuscript. All authors reviewed the results and approved the final version of the manuscript.

DECLARATION OF INTERESTS

Lihong L., S.I., J.Y., and D.D.H. are inventors on a provisional patent application on 10-40 described in this manuscript, titled “Isolation, characterization, and sequences of potent and broadly neutralizing monoclonal antibodies against SARS-CoV-2 and its variants as well as related coronaviruses” (63/271,627). D.D.H. is a co-founder of TaiMed Biologics and RenBio, consultant to WuXi Biologics and Brii Biosciences, and board director for Vicarious Surgical. Aubree Gordon serves on a scientific advisory board for Janssen Pharmaceuticals. Other authors declare no competing interests.

Reference:

1 Khare, S. *et al.* GISAID's Role in Pandemic Response. *China CDC Wkly* **3**, 1049-1051 (2021). https://doi.org:10.46234/ccdcw2021.255

2 WHO. *Statement on the fifteenth meeting of the IHR (2005) Emergency Committee on the COVID-19 pandemic*, <https://www.who.int/news/item/05-05-2023-statement-on-the-fifteenth-meeting-of-the-international-health-regulations-(2005)-emergency-committee-regarding-the-coronavirus-disease-(covid-19)-pandemic> (2023).

3 Wang, Q. *et al.* Antibody neutralisation of emerging SARS-CoV-2 subvariants: EG.5.1 and XBC.1.6. *Lancet Infect Dis* **23**, e397-e398 (2023). https://doi.org:10.1016/S1473-3099(23)00555-8

4 Wang, Q. *et al.* Alarming antibody evasion properties of rising SARS-CoV-2 BQ and XBB subvariants. *Cell* **186**, 279-286 e278 (2023). https://doi.org:10.1016/j.cell.2022.12.018

5 Miller, J. *et al.* Substantial Neutralization Escape by SARS-CoV-2 Omicron Variants BQ.1.1 and XBB.1. *N Engl J Med* **388**, 662-664 (2023). https://doi.org:10.1056/NEJMc2214314

6 Yue, C. *et al.* ACE2 binding and antibody evasion in enhanced transmissibility of XBB.1.5. *Lancet Infect Dis* **23**, 278-280 (2023). https://doi.org:10.1016/S1473-3099(23)00010-5

7 GOV.UK. *SARS-CoV-2 variant surveillance and assessment: technical briefing 53*, <https://www.gov.uk/government/publications/investigation-of-sars-cov-2-variants-technical-briefings/sars-cov-2-variant-surveillance-and-assessment-technical-briefing-53> (2023).

8 Wang, Q. *et al.* Evolving antibody evasion and receptor affinity of the Omicron BA.2.75 sublineage of SARS-CoV-2. *bioRxiv*, 2023.2003.2022.533805 (2023). https://doi.org:10.1101/2023.03.22.533805

9 Wang, Q. *et al.* Antibody evasion by SARS-CoV-2 Omicron subvariants BA.2.12.1, BA.4 and BA.5. *Nature* **608**, 603-608 (2022). https://doi.org:10.1038/s41586-022-05053-w

10 Liu, L. *et al.* Striking antibody evasion manifested by the Omicron variant of SARS-CoV-2. *Nature* **602**, 676-681 (2022). https://doi.org:10.1038/s41586-021-04388-0

11 Barnes, C. O. *et al.* SARS-CoV-2 neutralizing antibody structures inform therapeutic strategies. *Nature* **588**, 682-687 (2020). https://doi.org:10.1038/s41586-020-2852-1

12 Park, Y. J. *et al.* Antibody-mediated broad sarbecovirus neutralization through ACE2 molecular mimicry. *Science* **375**, 449-454 (2022). https://doi.org:10.1126/science.abm8143

13 Cao, Y. *et al.* Imprinted SARS-CoV-2 humoral immunity induces convergent Omicron RBD evolution. *Nature* (2022). https://doi.org:10.1038/s41586-022-05644-7

14 Nutalai, R. *et al.* Potent cross-reactive antibodies following Omicron breakthrough in vaccinees. *Cell* **185**, 2116-2131 e2118 (2022). https://doi.org:10.1016/j.cell.2022.05.014

15 Cao, Y. *et al.* Humoral immune response to circulating SARS-CoV-2 variants elicited by inactivated and RBD-subunit vaccines. *Cell Res* **31**, 732-741 (2021). https://doi.org:10.1038/s41422-021-00514-9

16 Zost, S. J. *et al.* Potently neutralizing and protective human antibodies against SARS-CoV-2. *Nature* **584**, 443-449 (2020). https://doi.org:10.1038/s41586-020-2548-6

17 Wang, K. *et al.* Memory B cell repertoire from triple vaccinees against diverse SARS-CoV-2 variants. *Nature* **603**, 919-925 (2022). https://doi.org:10.1038/s41586-022-04466-x

18 Zhou, B. *et al.* A broadly neutralizing antibody protects Syrian hamsters against SARS-CoV-2 Omicron challenge. *Nat Commun* **13**, 3589 (2022). https://doi.org:10.1038/s41467-022-31259-7

19 Wang, L. *et al.* Ultrapotent antibodies against diverse and highly transmissible SARS-CoV-2 variants. *Science* **373** (2021). https://doi.org:10.1126/science.abh1766
20 Pinto, D. *et al.* Cross-neutralization of SARS-CoV-2 by a human monoclonal SARS-CoV antibody. *Nature* **583**, 290-295 (2020). https://doi.org:10.1038/s41586-020-2349-y
21 Westendorf, K. *et al.* LY-CoV1404 (bebtelovimab) potently neutralizes SARS-CoV-2 variants. *Cell Rep* **39**, 110812 (2022). https://doi.org:10.1016/j.celrep.2022.110812
22 Liu, C. *et al.* The antibody response to SARS-CoV-2 Beta underscores the antigenic distance to other variants. *Cell Host Microbe* **30**, 53-68 e12 (2022). https://doi.org:10.1016/j.chom.2021.11.013
23 Cao, Y. *et al.* Rational identification of potent and broad sarbecovirus-neutralizing antibody cocktails from SARS convalescents. *Cell Rep* **41**, 111845 (2022). https://doi.org:10.1016/j.celrep.2022.111845
24 Liu, L. *et al.* An antibody class with a common CDRH3 motif broadly neutralizes sarbecoviruses. *Sci Transl Med*, eabn6859 (2022). https://doi.org:10.1126/scitranslmed.abn6859
25 Wang, Z. *et al.* Analysis of memory B cells identifies conserved neutralizing epitopes on the N-terminal domain of variant SARS-Cov-2 spike proteins. *Immunity* **55**, 998-1012 e1018 (2022). https://doi.org:10.1016/j.immuni.2022.04.003
26 Hong, Q. *et al.* Molecular basis of receptor binding and antibody neutralization of Omicron. *Nature* **604**, 546-552 (2022). https://doi.org:10.1038/s41586-022-04581-9
27 Guenthoer, J. *et al.* Identification of broad, potent antibodies to functionally constrained regions of SARS-CoV-2 spike following a breakthrough infection. *Proc Natl Acad Sci U S A* **120**, e2220948120 (2023). https://doi.org:10.1073/pnas.2220948120
28 Yuan, M. *et al.* A highly conserved cryptic epitope in the receptor binding domains of SARS-CoV-2 and SARS-CoV. *Science* **368**, 630-633 (2020). https://doi.org:10.1126/science.abb7269
29 Wang, Q. *et al.* Antigenic characterization of the SARS-CoV-2 Omicron subvariant BA.2.75. *Cell Host Microbe* (2022). https://doi.org:10.1016/j.chom.2022.09.002
30 Starr, T. N. *et al.* Deep Mutational Scanning of SARS-CoV-2 Receptor Binding Domain Reveals Constraints on Folding and ACE2 Binding. *Cell* **182**, 1295-1310 e1220 (2020). https://doi.org:10.1016/j.cell.2020.08.012
31 Qu, P. *et al.* Evasion of neutralizing antibody responses by the SARS-CoV-2 BA.2.75 variant. *Cell Host Microbe* **30**, 1518-1526 e1514 (2022). https://doi.org:10.1016/j.chom.2022.09.015
32 Han, P. *et al*. Receptor binding and complex structures of human ACE2 to spike RBD from omicron and delta SARS-CoV-2. *Cell* **185**, 630-640 e610 (2022). https://doi.org:10.1016/j.cell.2022.01.001
33 Lasrado, N. *et al.* Neutralization Escape by SARS-CoV-2 Omicron Subvariant BA.2.86. *bioRxiv*, 2023.2009.2004.556272 (2023). https://doi.org:10.1101/2023.09.04.556272
34 An, Y. *et al.* SARS-CoV-2 Omicron BA.2.86: less neutralization evasion compared to XBB sub-variants. *bioRxiv*, 2023.2009.2026.559580 (2023). https://doi.org:10.1101/2023.09.26.559580
35 Khan, K. *et al.* Evolution and neutralization escape of the SARS-CoV-2 BA.2.86 subvariant. *medRxiv*, 2023.2009.2008.23295250 (2023). https://doi.org:10.1101/2023.09.08.23295250
36 Yang, S. *et al.* Antigenicity and infectivity characterisation of SARS-CoV-2 BA.2.86. *Lancet Infect Dis* (2023). https://doi.org:10.1016/S1473-3099(23)00573-X
37 Uriu, K. *et al.* Transmissibility, infectivity, and immune evasion of the SARS-CoV-2 BA.2.86 variant. *Lancet Infect Dis* (2023). https://doi.org:10.1016/S1473-3099(23)00575-3
38 Sheward, D. J. *et al.* Sensitivity of the SARS-CoV-2 BA.2.86 variant to prevailing neutralising antibody

responses. *Lancet Infect Dis* (2023). https://doi.org:10.1016/S1473-3099(23)00588-1

39 Chalkias, S. *et al.* Safety and Immunogenicity of XBB.1.5-Containing mRNA Vaccines. *medRxiv*, 2023.2008.2022.23293434 (2023). https://doi.org:10.1101/2023.08.22.23293434

40 Zhang, J. *et al.* Structural impact on SARS-CoV-2 spike protein by D614G substitution. *Science* **372**, 525-530 (2021). https://doi.org:10.1126/science.abf2303

41 Parzych, E. M. *et al.* DNA-delivered antibody cocktail exhibits improved pharmacokinetics and confers prophylactic protection against SARS-CoV-2. *Nat Commun* **13**, 5886 (2022). https://doi.org:10.1038/s41467-022-33309-6

42 Zhou, T. *et al.* Structural basis for potent antibody neutralization of SARS-CoV-2 variants including B.1.1.529. *Science* **376**, eabn8897 (2022). https://doi.org:10.1126/science.abn8897

MATERIALS & METHODS

Human subjects

To evaluate neutralization sensitivity of BA.2.86 in this study, serum samples from three different clinical cohorts were utilized, which were "3 shots monovalent + 2 shots bivalent", "BA.2 breakthrough" and "XBB breakthrough" cohorts. Sera of the first cohort were from healthy donors who had received three doses of SARS-CoV-2 monovalent mRNA vaccines (either Moderna mRNA-1273 or Pfizer BNT162b2), followed by two doses of bivalent mRNA vaccines. The latter two consisted of patients who had a BA.2 and a XBB breakthrough infection after multiple vaccinations, respectively.

Eight BA.2 breakthrough samples studied in this project were collected at Columbia University Irving Medical Center by Michael T. Yin's and Magdalena E. Sobieszczyk's teams. The remaining samples were collected at the University of Michigan through the Immunity-Associated with SARS-CoV-2 Study (IASO), which is an ongoing cohort study in Ann Arbor, Michigan that began in 2020[ref.43]. All participants provided written informed consent and all serum samples were collected under protocols reviewed and approved by the Institutional Review Board of Columbia University or the Institutional Review Board of the University of Michigan Medical School.

IASO participants complete weekly symptom surveys and are tested for SARS-CoV-2 upon report of symptoms. All samples were examined by anti-nucleoprotein (NP) enzyme-linked immunosorbent assay (ELISA) to confirm status of prior SARS-CoV-2 infection. Infected strains were confirmed by sequencing.

Cell lines

HEK293T cells (CRL-3216) for pseudovirus generation and Vero-E6 cells (CRL-1586) for pseudovirus neutralization assays were purchased from the American Type Culture Collection (ATCC). Vero-ACE2-TMPRSS2 cells (NR-54970) for authentic virus neutralization assays were obtained from BEI Resources. Expi293 cells (A14527) used for protein expression and purification, were purchased from Thermo Fisher Scientific. All cells were maintained according to the manufacturers' instructions. The morphology of each cell line was confirmed visually before use. All cell lines tested negative for mycoplasma. Vero-E6 cells are from African green monkey kidneys. HEK293T cells and Expi293 cells are of female origin.

Antibody and spike protein purification

To make antibodies and hACE2 with a Fc tag, the constructs encoding heavy and light chains of each antibody and the construct encoding hACE2 with Fc tag were/was transfected into Expi293 cells using 1 mg/mL polyethylenimine (PEI), respectively. Five days post transfection, cell supernatants were collected and clarified, and the expressed antibody and hACE2-Fc in cell supernatants were purified by using rProtein A Sepharose (GE).

The soluble spike constructs were transfected into Expi293 cells using 1 mg/mL polyethylenimine (PEI). Five days post transfection, cell supernatants were collected and clarified, and the spike proteins with a His tag were purified from the supernatant by using nickel-nitrilotriacetic acid (Ni-NTA) Sepharose (GE).

Construction of SARS-CoV-2 spike plasmids

Spike-expressing plasmids for BA.2, XBB.1.5, and EG.5.1 pseudovirus generation were made in the previous studies[3,44,45]. Spike-expressing plasmids of BA.2.86-V1 and BA.2.86-V2 variants, as well as individual mutations found in BA.2.86 in the BA.2 background, were generated by MEGAA[46] as previously described[4,10]. Briefly, 5'-phosphorylated oligo pools with designed mutations were synthesized from SYNTAX Platform (Model STX-200) and Integrated DNA Technologies. The corresponding regions of the BA.2 spike gene construct were replaced with oligos by using annealing, extension, ligation, and PCR steps. To confirm the sequences of the variants, next generation sequencing[47] and Oxford Nanopore sequencing were performed on the Illumina Miseq platform (single-end mode with 50 bp R1) and on a MinION with the MinKNOW v21.11.8 (Oxford Nanopore Technologies). Using Cutadapt v2.1 [ref.48], Bowtie2 v2.3.4 [ref.49], Guppy v3.6.0 (Oxford Nanopore Technologies) in GPU mode, and a custom Python script, we trimmed, aligned, basecalled, and filtered the reads for the full-length spike genes , respectively, and then viewed the read alignments in Integrative Genomics Viewer[50].

To make soluble spike proteins of SARS-CoV-2 variants investigated in this study, we generated plasmid constructs encoding ectodomains (1-1208aa based on the sequence numbering of WA1) of spike proteins. In addition, these constructs also have a GSAS substitution at furin cleavage site (682-685aa which are RRAR in WA1) and a 2P substitution at positions K986 and V987 and are fused with a foldon tag followed by a 6× His tag. All constructs were confirmed by Sanger sequencing.

Pseudovirus production

To make SARS-CoV-2 pseudoviruses, the spike-expressing plasmids were transfected into HEK293T cells using 1 mg/mL PEI. One day post transfection, cells were infected with VSV-G pseudotyped ΔG-luciferase (G*ΔG-luciferase, Kerafast) at a multiplicity (MOI) of ~3 to 5. Two hours after infection, VSV-G pseudotyped ΔG-luciferase was removed by washing the cells with PBS three times. Cells were then maintained in fresh medium for another day before the cell supernatants containing pseudoviruses were harvested, clarified by centrifugation, aliquoted, and stored at -80°C.

Pseudovirus neutralization assay

Before conducting neutralization assays, pseudoviruses were titrated on Vero-E6 cells to normalize the viral input between different viruses and assays. Serum samples were inactivated at 56˚C for 30 minutes before use. For serum neutralization assays, inactivated sera were diluted from 12.5-fold with a dilution factor of four. For mAb neutralization assays, mAbs were diluted from

20 µg/mL with a dilution factor of five. Dilutions were performed in 96 well plates in triplicates. Then 50 µL of each dilution of serum or mAb was incubated with 50 µL diluted pseudovirus for 1 hour at 37˚C, followed by adding 100 µL of resuspended Vero-E6 cells at a density of 4×10^6 cells/mL. Wells with no serum or no mAb (meaning virus alone) were included in all plates. Plates were then incubated at 37˚C overnight before luciferase activity was quantified using the Luciferase Assay System (Promega) on SoftMax Pro v.7.0.2 (Molecular Devices). The reduction in luciferase activity for each serum and mAb dose, when compared with the "virus alone" controls, was calculated. Neutralization ID_{50} values for sera and IC_{50} values for mAbs were obtained by fitting a nonlinear five-parameter dose-response curve to the data in GraphPad Prism v.10.0.2.

Authentic virus neutralization assay

The SARS-CoV-2 viruses hCoV-19/USA/MD-HP47946/2023 (EG.5.1) (Cat # NR-59576) and an isolate of hCoV-19/USA/MI-UM-10052670540/2023 (BA2.86) bearing an additional adaptation spike mutation, G35V, and a mutation in E protein (V14del) were obtained from BEI Resources (NIAID, NIH) and propagated by passaging in Vero-ACE2-TMPRSS2 cells. Virus infectious titers were determined by an end-point dilution and cytopathogenic effects on Vero-TMPRSS2 cells instead of using Vero-E6 cells as previously described[51].

An end-point dilution microplate neutralization assay was performed to measure the neutralization activity of sera from vaccinated and boosted individuals as earlier[9]. Briefly, five-fold serial dilutions of serum samples were made in EMEM containing 10% fetal bovine serum and incubated with each of the viruses tested at 37˚C/5% CO_2 for 1h. The mix was then overlaid on an overnight culture of Vero-ACE2-TMPRSS2 cells to attain a final MOI 0.2. Reaction was incubated at 37˚C/5% CO_2 for 48h. Virus induced cytopathic effects were visually scored for each well in a blinded manner by two independent observers. The results were then converted into the percentage of neutralization at a given sample dilution, and the data were plotted using a five-parameter dose-response curve in GraphPad Prism v.10.0.2.

Phylogenetic analysis

Genome sequences of SARS-CoV-2 subvariants were retrieved from the GISAID (global initiative on sharing avian flu data) database. Subsequently, the spike protein sequences were extracted from the genomes using an in-house python script. The spike protein sequences were then aligned using the MUSCLE software (version 3.8.31). Low-quality sequencing sites characterized by the presence of 'N' were manually curated to ensure the mutations fit the consensus mutations in each variant. A Maximum Likelihood phylogenetic tree was constructed using MEGA11, utilizing the Tamura-Nei model and validated with 500 bootstrap replications.

Antigenic cartography

Antigenic distances between sera to BA.2 and other SARS-CoV-2 variants were determined by integrating ID_{50} values of individual serum samples through a published antigenic cartography approach[52]. The visualization was generated using the Racmacs package (v.1.1.4, https://acorg.github.io/Racmacs/) in R version 4.0.3. With optimization steps set at 2,000 and the

minimum column basis parameter set to 'none', the 'mapDistances' function was employed to calculate antigenic distances between each serum sample and variant. The final distances were represented by the average distances from all sera to each variant. BA.2 served as the center of sera for each group, the seeds for each antigenic map were manually adjusted to ensure that EG.5.1 was displayed in the horizontal direction relative to BA.2.

Structural modeling

The structures of antibody–RBD complexes for modeling were obtained from PDB (PDB IDs: 7WKA for S3H3, 8D8Q for COV2-2130, 7MMO for LY-CoV1404, 7TAS for S2K146, and 7TCA for A19-46.1). The electrostatic potential was estimated by APBS electrostatics plugin, and the mutagenesis analysis were performed by Pymol version 2.5.4 (Schrödinger, LLC). The PDB ID for the BA.2 RBD and hACE2 complex is 7ZF7. The interaction residues of footprints were identified by PDBePISA[53].

Surface plasmon resonance (SPR)

The CM5 chip was immobilized with anti-His antibodies utilizing the His Capture Kit (Cytiva) to facilitate the capture of the spike protein via its C-terminal His-tag. Thereafter, a serial dilution of the hACE2 protein fused with a Fc tag was introduced over the chip, prepared in the HBS-EP+ buffer (Cytiva). Binding affinities were ascertained using the Biacore T200 system, operating at 25˚C in a single-cycle mode. Subsequently, the acquired data were scrutinized using the Evaluation Software, adhering to a 1:1 binding model.

Quantification and statistical analysis

IC_{50} and ID_{50} values were determined by fitting the data to five-parameter dose-response curves in GraphPad Prism v.10.0.2. Comparisons were made by two-tailed Wilcoxon matched-pairs signed-rank tests.

Data availability

All experimental data are provided in the manuscript. Materials used in this study will be available under an appropriated Materials Transfer Agreement. Antigenic maps were generated using the Racmacs package (v.1.1.4, https://acorg.github.io/Racmacs/) in R version 4.0.3. SARS-CoV-2 spike sequences were downloaded from the global initiative on sharing all influenza data (GISAID) (https://www.gisaid.org/). The structures used for analysis in this study are available from PDB under IDs 7KRR, 7WKA, 8D8Q, 7MMO, 7TAS, 7TCA, and 7ZF7.

Methods reference:

43 Simon, V. *et al.* PARIS and SPARTA: Finding the Achilles' Heel of SARS-CoV-2. *mSphere* **7**, e0017922 (2022). https://doi.org:10.1128/msphere.00179-22

44 Iketani, S. *et al.* Antibody evasion properties of SARS-CoV-2 Omicron sublineages. *Nature* **604**, 553-556 (2022). https://doi.org:10.1038/s41586-022-04594-4

45 Wang, Q. *et al.* Deep immunological imprinting due to the ancestral spike in the current bivalent COVID-19 vaccine. *bioRxiv*, 2023.2005.2003.539268 (2023). https://doi.org:10.1101/2023.05.03.539268

46 Liu, L., Huang, Y. & Wang, H. H. Fast and efficient template-mediated synthesis of genetic variants. *Nat Methods* **20**, 841-848 (2023). https://doi.org:10.1038/s41592-023-01868-1

47 Baym, M. *et al.* Inexpensive multiplexed library preparation for megabase-sized genomes. *PLoS One* **10**, e0128036 (2015). https://doi.org:10.1371/journal.pone.0128036

48 Martin, M. Cutadapt removes adapter sequences from high-throughput sequencing reads. *2011* **17**, 3 (2011). https://doi.org:10.14806/ej.17.1.200

49 Langmead, B. & Salzberg, S. L. Fast gapped-read alignment with Bowtie 2. *Nat Methods* **9**, 357-359 (2012). https://doi.org:10.1038/nmeth.1923

50 Robinson, J. T. *et al.* Integrative genomics viewer. *Nat Biotechnol* **29**, 24-26 (2011). https://doi.org:10.1038/nbt.1754

51 Liu, L. *et al.* Potent neutralizing antibodies against multiple epitopes on SARS-CoV-2 spike. *Nature* **584**, 450-456 (2020). https://doi.org:10.1038/s41586-020-2571-7

52 Smith, D. J. *et al.* Mapping the antigenic and genetic evolution of influenza virus. *Science* **305**, 371-376 (2004). https://doi.org:10.1126/science.1097211

53 Krissinel, E. & Henrick, K. Inference of macromolecular assemblies from crystalline state. *J Mol Biol* **372**, 774-797 (2007). https://doi.org:10.1016/j.jmb.2007.05.022

Extended Data table and figure legends

Extended Data Table 1. Demographics of clinical cohorts. Demographics and vaccination/infection information for serum samples used in this study.

Extended Data Table 2. Neutralization activity of mAbs against the indicated viruses. Neutralization IC_{50} values of BA.2, XBB.1.5, EG.5.1, BA.2.86-V1 and BA.2 carrying individual spike mutations found in BA.2.86 by mAbs.

Extended Data Table 3. Neutralization activity of mAbs against BA.2.86 carrying back mutations. Neutralization IC_{50} values of BA.2.86-V1 carrying individual reverse mutations of L50S, V332I, K403R, and Q493R by mAbs.

Extended Data Figure 1. Spike sequence alignment of WA1 and BA.2 with BA.2.86 from human cases deposited to GISAID as of September 5, 2023. The sequence numbering is based on WA1. Red boxes indicate the alignments of amino acids at position 16 and 670. "X", low-quality sequencing data.

Extended Data Figure 2. Serum neutralization of authentic BA.2.86 compared with EG.5.1. Neutralizing ID_{50} titers of serum samples from "XBB breakthrough" cohort against authentic BA.2.86 and EG.5.1. The geometric mean ID_{50} titers (GMT) are presented above symbols. The neutralization assay limit of detection (dotted line) is 100. Statistical analysis was performed by employing Wilcoxon matched-pairs signed-rank test. GMT of BA.2.86 is around 1.2-fold (1.2X) higher than that of EG.5.1. n, sample size. dpi, days post infection.

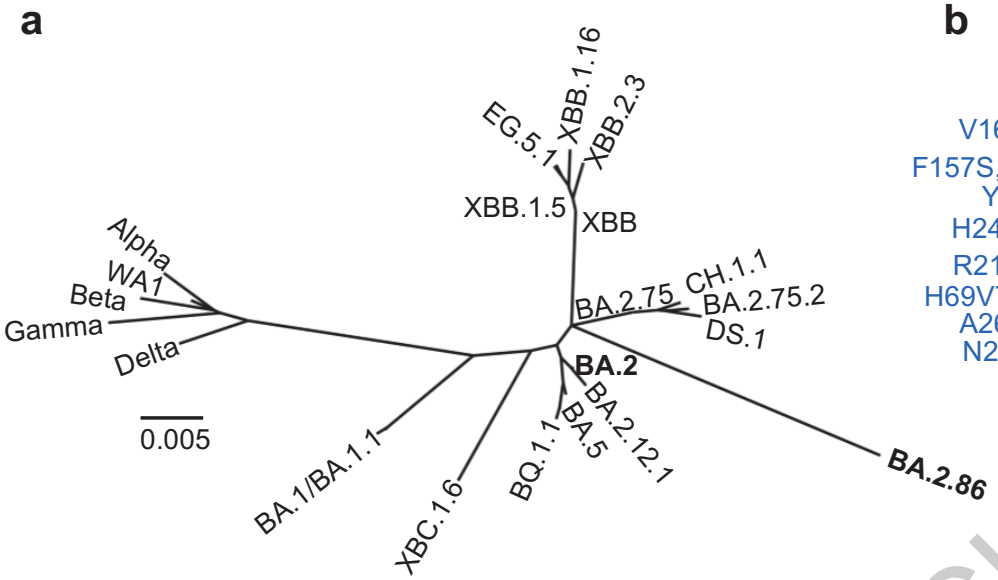

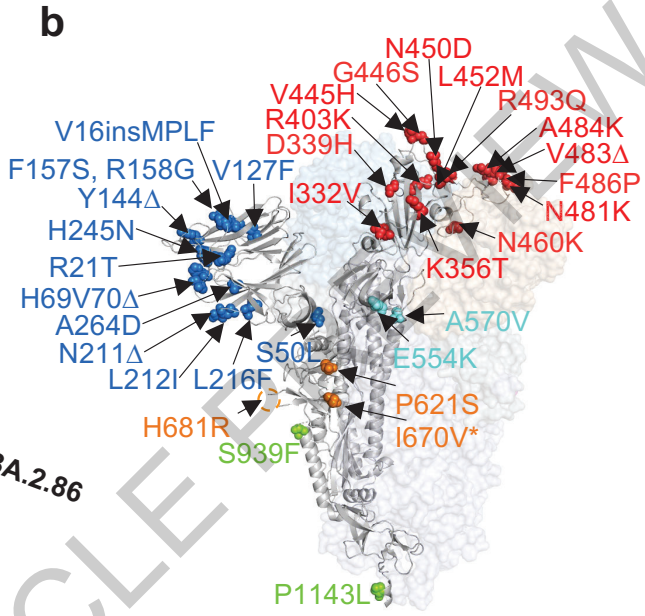

c

Spike Mutations on BA.2	NTD													RBD																	SD1		SD2			S2	
	V16ins	R21	S50	H69V70	V127	Y144	F157	R158	N211	L212	L216	H245	A264	I332	D339	K356	R403	V445	G446	N450	L452	N460	N481	V483	A484	F486	R493	E554	A570	P621	I670	H681	S939	P1143
BA.2.86-V1	MPLF	T	L	Δ	F	Δ	S	G	Δ	I	F	N	D	V	H	T	K	H	S	D	W	K	K	Δ	K	P	Q	K	V	S		R	F	L
BA.2.86-V2	MPLF	T	L	Δ	F	Δ	S	G	Δ	I	F	N	D	V	H	T	K	H	S	D	W	K	K	Δ	K	P	Q	K	V	S	V	R	F	L
Alpha				Δ		Δ																														
Beta																									K										
Gamma																									K										
Delta							Δ	Δ													R											R			
BA.1				Δ		Δ			Δ	Δ									S																
BA.2.12.1																					Q														
BA.4/5				Δ																	R					V	Q								
BQ.1				Δ																	R	K				V	Q								
BA.2.75							L								H				S			K					Q								
DS.1							L								H	T	K		S			K				S	Q								
XBB.1						Δ									H			P	S			K				S	Q								
XBB.1.5						Δ									H			P	S			K				P	Q								
EG.5.1						Δ									H			P	S			K				P	Q								

a

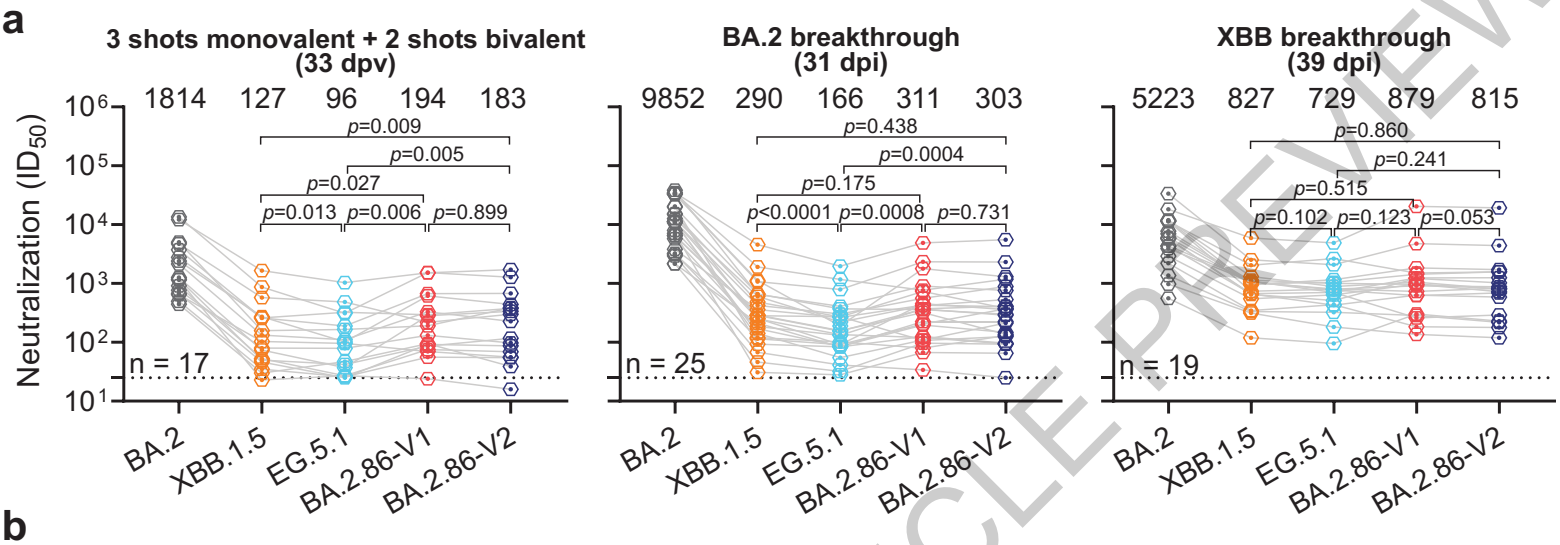

b

Fold change in geometric mean ID50 titer	Relative to BA.2			Relative to XBB.1.5			Relative to EG.5.1		
	XBB.1.5	EG.5.1	BA.2.86-V1	BA.2	EG.5.1	BA.2.86-V1	BA.2	XBB.1.5	BA.2.86-V1
3 shots monovalent + 2 shots bivalent	14	19	9.4	14	1.3	1.5	19	1.3	2.0
BA.2 breakthrough	34	60	32	34	1.8	1.1	60	1.8	1.9
XBB breakthrough	6	7	6	6.3	1.1	1.1	7.2	1.1	1.2

c

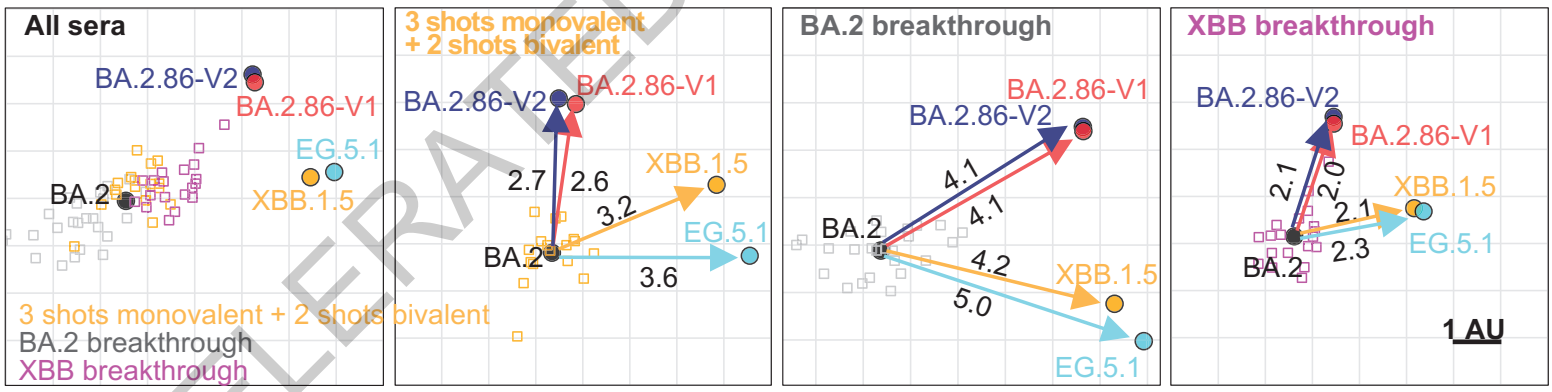

a

Fold change in IC50 compared with BA.2	NTD	NTD-SD2	SD1				RBD class 1								RBD class 2				RBD class 3					RBD class 4/1		
	C1520	C1717	S3H3	C68.59	ADARC1	ADARC2	S2K146	BD57-0129	BD56-1302	BD56-1854	Omi-3	Omi-18	BD-515	Omi-42	COV2-2196	XGv347	ZCB11	XGv051	A19-46.1	S309	COV2-2130	LY-COV1404	Beta-54	BD55-4637	SA55	10-40
XBB.1.5	>6973	-1.3	-1.6	1.2	1.2	-1.2	2.6	1.7	4.8	5.2	34	593	13	-1.7	>81	>7505	>2293	345	>223	-1.4	>1574	>10000	2.4	4.8	1.8	-1.0
EG.5.1	>6973	1.7	1.3	1.2	1.9	1.4	1.4	1.1	4.9	9.4	>888	>2921	>807	325	>81	>7505	>2293	589	>223	-2.6	>1574	>10000	2.2	2.8	1.4	-1.4
BA.2.86-V1	150	1.5	>639	>219	>115	160	>254	1.1	2.5	1.3	40	152	9.3	-1.3	>81	>7505	>2293	>10142	>223	19	>1574	>10000	>68	-1.2	-9.6	-4.4
BA.2-V16insMPLF	2.0	1.7	-1.6	-1.3	-1.0	-2.3	1.4	2.4	2.0	2.1	2.3	1.5	1.2	1.5	1.8	1.9	4.2	1.6	-1.8	-1.4	1.2	-1.1	2.5	1.1	1.5	1.3
BA.2-R21T	1.1	-1.3	-1.1	-2.1	-1.0	1.2	-1.2	1.5	1.2	1.3	1.7	1.2	-1.1	1.4	1.5	1.8	3.7	1.1	-1.0	-1.1	-1.1	-1.9	1.8	1.6	1.4	-1.7
BA.2-S50L	-1.3	-2.4	1.1	-1.6	-2.3	1.6	-5.9	-1.5	-1.1	1.3	-2.0	-2.0	-2.9	-2.1	-1.2	/	/	/	-5.9	-2.9	-2.3	-1.3	-2.8	-2.3	-3.1	-7.1
BA.2-H60/V70Δ	-1.3	1.1	-1.0	1.2	-1.2	-1.0	-1.1	1.3	1.4	2.3	1.2	-1.3	-2.1	1.2	1.4	-1.0	1.8	/	-1.4	-1.2	-1.1	-1.2	1.1	-1.2	-1.1	1.3
BA.2-V127F	-1.3	1.1	-1.5	-1.9	-1.4	2.5	-1.5	1.6	1.3	1.9	1.3	1.2	-1.3	1.2	2.0	1.6	1.9	1.6	1.1	-1.1	1.3	/	1.7	1.2	1.2	1.1
BA.2-Y144Δ	-1.3	-1.2	-1.3	-1.0	-1.3	-1.2	-1.5	2.3	2.3	1.1	1.7	1.9	1.0	1.3	1.9	2.1	2.8	1.8	-1.9	-1.2	1.2	-1.5	1.5	1.3	1.5	1.3
BA.2-F157S	-1.3	-1.2	-1.5	-1.5	-0.9	-1.2	-1.3	1.1	1.4	1.4	1.3	1.1	-1.5	1.1	-1.0	-1.1	-1.6	1.0	-1.5	-1.6	-1.8	-1.3	1.4	-1.3	-1.1	-1.1
BA.2-R158G	-1.3	-1.8	-1.9	-1.5	-1.1	-1.3	-1.2	2.4	1.6	1.5	1.1	-1.2	-2.1	-1.5	1.3	-1.0	1.8	/	-1.5	-1.8	1.1	-1.3	1.9	-1.3	1.3	-1.2
BA.2-N211Δ	-1.3	-2.6	-1.8	-1.2	-0.9	-1.2	-2.7	-1.1	1.3	1.3	1.2	-1.0	-1.5	1.3	-1.2	-1.9	-1.2	/	-1.5	-2.1	-1.2	-1.0	1.4	-1.8	-1.1	-2.1
BA.2-L212I	-1.3	1.1	-1.4	-1.0	-1.3	-1.1	1.1	1.2	1.3	1.5	1.3	-2.1	-1.7	-1.0	1.6	-1.7	1.6	/	-1.1	-2.3	-1.2	-1.3	1.6	-1.5	1.3	-1.4
BA.2-L216F	-1.3	1.5	1.0	-1.1	-0.8	-1.2	-1.7	1.1	-1.1	1.1	1.0	-1.1	-1.8	-1.2	1.5	1.5	2.0	1.3	-1.1	-1.3	-1.2	-1.7	1.2	-1.5	-1.3	-1.3
BA.2-H245N	111	1.1	-1.2	1.1	-0.8	2.6	1.1	1.5	1.4	1.6	1.3	1.3	-1.3	1.0	1.5	1.8	2.0	1.6	-1.0	1.0	1.2	/	1.6	1.0	1.2	-1.1
BA.2-A264D	-1.3	-1.3	-1.3	-1.2	-1.1	-1.2	1.0	1.1	1.3	1.0	1.5	1.1	-1.4	-1.3	1.3	1.6	1.5	1.2	-1.5	-1.3	1.3	/	1.6	-1.2	-1.1	-1.4
BA.2-I332V	-1.3	-1.2	1.1	1.4	-0.9	3.5	-2.8	-1.8	-1.8	-1.4	-2.3	-2.1	-2.3	-2.3	-1.2	/	-14	1.3	-2.8	1.8	-1.7	-1.3	-1.4	-1.8	-2.7	-5.3
BA.2-D339H	-1.3	1.6	-1.1	-1.5	-1.4	-1.6	-1.0	2.0	1.6	1.8	1.6	1.5	-1.1	1.0	1.6	-1.1	2.2	1.2	-1.3	-4.6	-1.4	-1.0	2.9	1.0	1.4	1.0
BA.2-K356T	-1.3	-1.0	-2.6	-1.8	-1.2	-2.1	1.2	3.0	2.1	2.7	3.3	1.5	1.1	1.6	3.0	1.1	3.2	1.0	7.5	20	1.2	-1.6	-1.3	2.7	2.6	1.3
BA.2-R403K	1.1	-2.6	1.2	1.3	-1.0	5.0	-3.5	-1.7	-1.3	-1.7	-3.1	-1.8	-4.1	-3.0	-1.3	/	-2.0	/	-1.7	-2.0	-1.2	1.4	-2.0	-4.0	-4.2	-4.5
BA.2-V445H	-1.3	-1.7	-1.4	-2.0	-1.5	-1.5	-1.3	1.1	1.1	1.0	1.1	1.3	-1.4	-1.0	1.1	1.6	3.3	-1.6	-1.1	-1.2	-1.2	>10000	>68	1.6	-3.7	1.0
BA.2-G446S	-2.2	-1.4	-2.1	-1.4	-1.2	-1.5	-2.5	-1.1	-1.2	1.1	-1.1	-1.2	-1.5	-1.3	1.9	-1.6	1.5	-1.2	1.4	-1.5	1.1	1.3	-14	1.2	-1.5	-1.7
BA.2-N450D	-1.2	1.6	-1.4	-1.9	-1.0	-1.1	-2.0	1.3	1.4	1.8	1.1	1.1	-1.5	-1.0	1.0	-1.5	1.6	-1.8	5.3	-1.6	242	1.1	-1.3	-1.2	1.2	1.2
BA.2-L452W	-1.2	1.4	-1.1	-1.8	-1.4	1.1	-1.2	1.4	1.0	1.7	1.7	1.0	-1.8	-1.2	1.5	-1.3	1.7	1.6	>223	1.2	1.4	-1.6	2.6	1.3	1.3	1.0
BA.2-N460K	-1.3	-1.1	-2.5	1.1	-0.8	-1.8	1.9	3.1	4.1	3.0	34	4.5	8.4	3.1	-1.5	/	3.4	2.0	1.4	-1.7	1.1	-1.2	2.5	2.0	1.6	1.3
BA.2-N481K	1.3	-1.0	-1.1	-1.1	-1.3	1.4	-1.5	1.6	1.3	1.6	1.3	-1.2	-1.6	-1.0	2.7	2.4	2.4	1.3	1.1	-1.6	1.3	-1.5	1.4	-1.3	-1.3	-1.0
BA.2-V483Δ	1.2	1.1	-1.3	-1.6	-1.2	1.1	-1.2	1.2	-1.0	1.3	1.6	-1.2	-1.4	-1.0	1.5	2.1	1.5	1.3	1.6	-1.1	-1.1	-1.6	1.1	1.2	1.2	1.0
BA.2-A484K	1.0	-1.1	-1.7	-1.4	-1.4	-1.2	10	1.6	1.5	1.6	1.4	-1.6	-1.0	1.4	2.4	1.4	1.3	1.1	17	-1.2	1.1	-1.5	-1.2	-1.1	-1.1	-1.1
BA.2-F486P	-2.1	-1.2	-1.5	-1.4	-1.7	-1.3	>254	1.6	2.7	3.7	26	2.2	1.4	1.8	>81	>7505	>2293	298	-1.2	-1.7	-1.1	-1.5	1.4	1.5	-1.0	1.3
BA.2-R493Q	2.1	-2.3	-1.0	1.2	-1.1	-1.1	-11	-2.8	-2.2	-1.5	-1.7	1.2	-3.7	-5.2	-27	/	/	/	-2.2	1.4	-1.2	-1.4	-1.4	-1.2	-2.1	-1.7
BA.2-E554K	-1.3	-1.1	>639	>219	>115	6.0	-1.4	1.4	1.5	1.4	1.2	-1.3	-1.3	-1.5	1.1	1.1	1.5	1.0	-1.4	-1.7	1.2	/	1.5	-1.4	1.0	-1.3
BA.2-A570V	-1.3	-2.4	-1.6	-2.5	-1.7	-1.8	-1.5	1.3	1.0	-1.4	1.1	1.2	-1.5	-1.4	1.4	1.4	1.4	1.1	-1.5	-1.5	-1.2	/	1.7	-1.1	-1.1	-1.2
BA.2-P621S	-1.3	-1.1	3.7	-1.2	1.3	-1.6	-1.8	-1.0	-1.2	-1.3	1.1	-2.1	-1.8	-1.9	2.5	1.1	1.4	-1.4	-1.3	-2.1	-1.7	/	-1.2	-1.4	1.3	-2.6
BA.2-I670V	-1.3	-1.5	-1.7	-1.3	-1.8	-1.8	-1.1	1.5	1.3	1.2	1.3	1.1	-1.6	-1.1	1.3	1.3	1.6	1.3	-1.2	-1.5	1.1	-1.7	1.6	1.0	-1.1	-1.2
BA.2-H681R	-2.1	-1.5	-1.9	-1.2	-1.4	-1.6	-2.1	1.4	1.0	1.0	1.3	1.2	-1.7	-1.3	1.1	-1.8	1.5	1.2	-1.1	-1.3	1.0	-1.5	1.5	-1.0	1.2	1.1
BA.2-S939F	-1.6	1.1	-2.0	-2.5	-1.3	-1.2	-2.4	-1.4	-1.0	1.2	-1.1	-1.2	-2.6	-1.5	1.3	-1.2	-1.5	-1.3	-2.4	-1.7	-1.1	-1.4	1.2	-1.5	-1.3	-2.7
BA.2-P1143L	-1.3	-1.3	-1.6	-1.8	-1.8	-1.7	-2.7	1.2	1.1	1.2	-1.0	-1.3	-2.5	-1.5	-1.2	-1.2	-1.6	-1.3	-2.1	-2.2	1.0	-1.8	1.8	-1.2	1.0	-1.6

<-10 | <-3 | -3 to 3 | >3 | >10 | >100

b

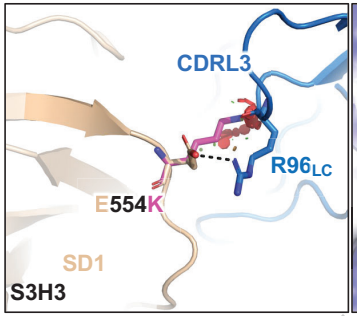

c

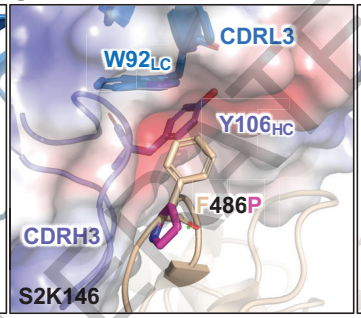

d

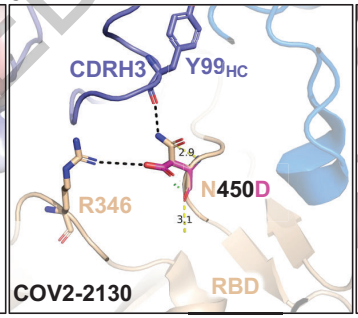

e

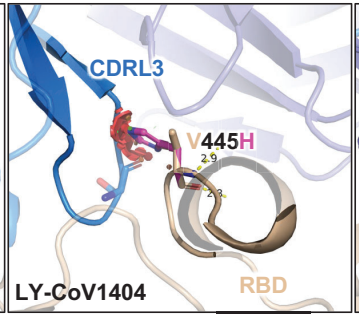

f

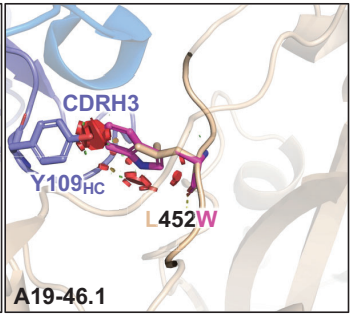

g

Fold change in IC50 compared with BA.2.86-V1	RBD class 1				RBD class 4/1		
	BD56-1302	BD56-1854	Omi-3	Omi-42	BD55-4637	SA55	10-40
BA.2.86-L50S	1.6	1.7	3.9	2.8	2.1	1.1	1.6
BA.2.86-V332I	2.1	1.8	1.1	1.9	2.5	1.3	4.2
BA.2.86-K403R	1.9	2.5	8.4	3.9	4.5	3.1	2.3
BA.2.86-Q493R	1.6	3.9	>34	1.9	2	1.5	-1.4

Sensitization — Resistance

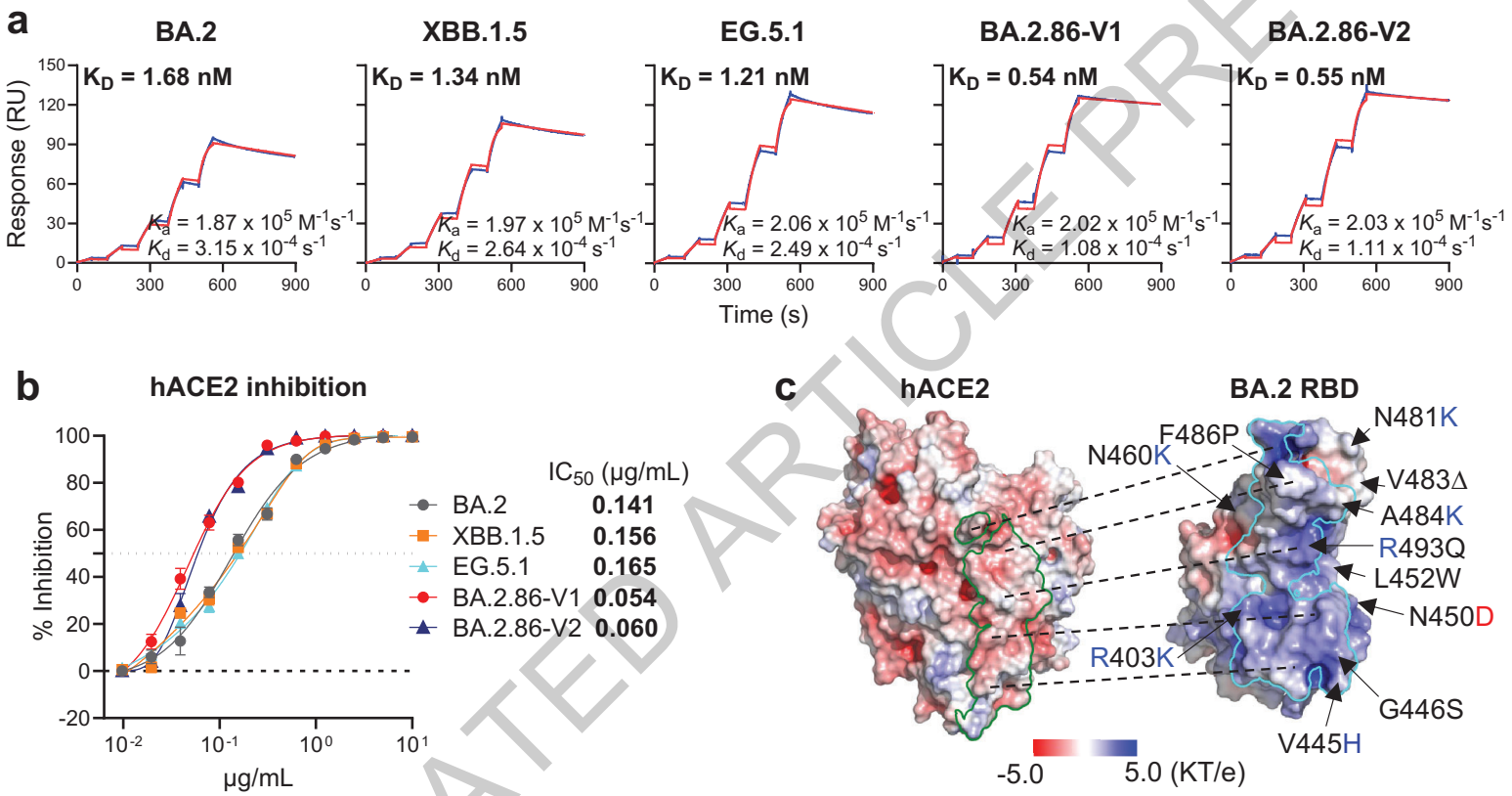

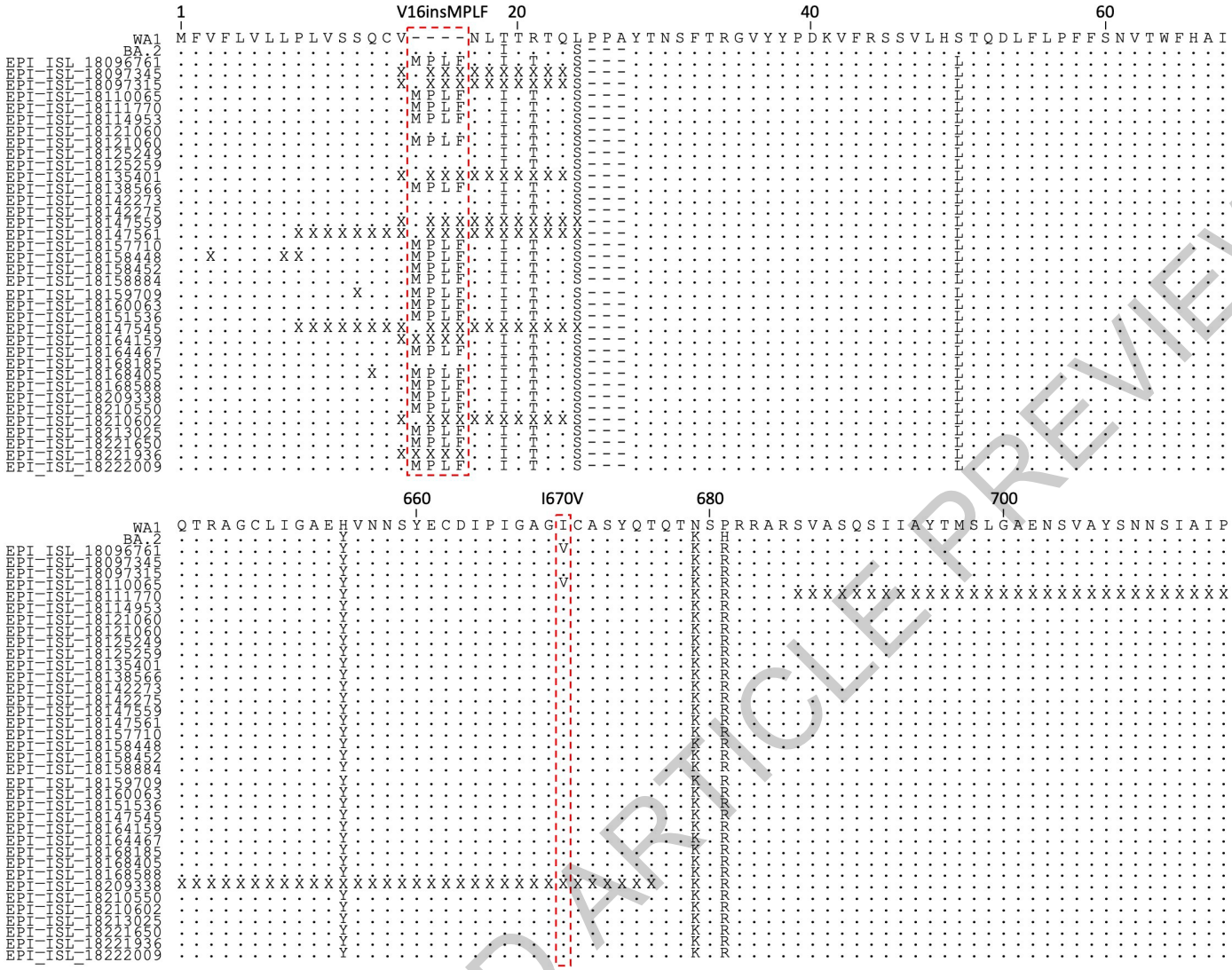

Extended Data Fig. 1

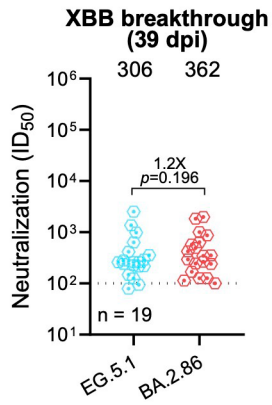

Extended Data Fig. 2

Sample ID	Vaccine type and infected strain	Days post last vaccination or *infection	Documented COVID-19	Age	Gender
3 shots monovalent + 2 shots bivalent (n = 17)					
L1	BNT162b2/BNT162b2/BNT162b2/BNT162b2/Pfizer Bivalent/Pfizer Bivalent	33	No	66	Female
L2	BNT162b2/BNT162b2/BNT162b2/BNT162b2/Pfizer Bivalent/Pfizer Bivalent	31	No	68	Male
L3	BNT162b2/BNT162b2/BNT162b2/BNT162b2/Pfizer Bivalent/Pfizer Bivalent	28	No	74	Male
L4	BNT162b2/BNT162b2/BNT162b2/BNT162b2/Pfizer Bivalent/Pfizer Bivalent	32	No	64	Female
L5	BNT162b2/BNT162b2/BNT162b2/BNT162b2/Pfizer Bivalent/Pfizer Bivalent	33	No	64	Female
L6	BNT162b2/BNT162b2/BNT162b2/BNT162b2/Pfizer Bivalent/Pfizer Bivalent	34	No	65	Female
L7	BNT162b2/BNT162b2/BNT162b2/BNT162b2/Pfizer Bivalent/Pfizer Bivalent	29	No	70	Male
L8	mRNA-1273/mRNA-1273/mRNA-1273/mRNA-1273/Moderna Bivalent/Pfizer Bivalent	33	No	63	Male
L9	BNT162b2/BNT162b2/BNT162b2/BNT162b2/Pfizer Bivalent/Pfizer Bivalent	33	No	63	Male
L10	AstraZeneca/AstraZeneca/BNT162b2/BNT162b2/Pfizer Bivalent/Pfizer Bivalent	43	No	73	Male
L11	BNT162b2/BNT162b2/BNT162b2/BNT162b2/Pfizer Bivalent/Pfizer Bivalent	34	No	66	Male
L12	BNT162b2/BNT162b2/BNT162b2/BNT162b2/Pfizer Bivalent/Pfizer Bivalent	26	No	78	Male
L13	BNT162b2/BNT162b2/BNT162b2/BNT162b2/Pfizer Bivalent/Pfizer Bivalent	33	No	68	Female
L15	BNT162b2/BNT162b2/BNT162b2/BNT162b2/Pfizer Bivalent/Pfizer Bivalent	31	No	74	Male
L16	BNT162b2/BNT162b2/BNT162b2/BNT162b2/Pfizer Bivalent/Pfizer Bivalent	46	No	94	Male
L17	BNT162b2/BNT162b2/BNT162b2/BNT162b2/Moderna Bivalent/Pfizer Bivalent	21	No	64	Female
L18	mRNA-1273/mRNA-1273/mRNA-1273/mRNA-1273/Moderna Bivalent/Moderna Bivalent	42	No	60	Female
BA.2 breakthrough (n = 25)					
Q35	BNT162b2/BNT162b2/BA.2	*14	Yes	50	Female
Q36	BNT162b2/BNT162b2/BNT162b2/Ad26.COV2.S/BA.2	*22	Yes	69	Male
Q50	mRNA-1273/mRNA-1273/mRNA-1273/BA.2	*14	Yes	34	Male
Q51	BNT162b2/BNT162b2/mRNA-1273/BA.2	*19	Yes	33	Female
Q52	BNT162b2/BNT162b2/mRNA-1273/BA.2	*18	Yes	29	Female
C1	BNT162b2/BNT162b2/BNT162b2/BA.2	*28	Yes	22	Male
C2	mRNA-1273/mRNA-1273/mRNA-1273/BA.2	*56	Yes	30	Female
C3	BNT162b2/BNT162b2/BNT162b2/BA.2	*34	Yes	30	Female
BA.2-10	BNT162b2/BNT162b2/mRNA-1273/BA.2	*30	Yes	59	Female
BA.2-11	BNT162b2/BNT162b2/BNT162b2/BA.2	*29	Yes	39	Female
BA.2-12	BNT162b2/BNT162b2/BNT162b2/BA.2	*18	Yes	45	Female
BA.2-13	BNT162b2/BNT162b2/BNT162b2/BNT162b2/BA.2	*31	Yes	59	Female
BA.2-14	BNT162b2/BNT162b2/BNT162b2/BNT162b2/BA.2	*25	Yes	39	Male
BA.2-15	BNT162b2/BNT162b2/BNT162b2/mRNA-1273/BA.2	*32	Yes	61	Male
BA.2-16	Ad26.COV2.S/Ad26.COV2.S/BA.2	*29	Yes	47	Female
BA.2-17	BNT162b2/BNT162b2/BNT162b2/BA.2	*29	Yes	45	Male
BA.2-18	BNT162b2/BNT162b2/BNT162b2/mRNA-1273/BA.2	*29	Yes	25	Male
BA.2-19	BNT162b2/BNT162b2/BNT162b2/BA.2	*32	Yes	37	Female
BA.2-20	BNT162b2/BNT162b2/BNT162b2/BNT162b2/BA.2	*31	Yes	62	Male
BA.2-21	BNT162b2/BNT162b2/BNT162b2/mRNA-1273/BNT162b2/BA.2	*28	Yes	58	Male
BA.2-22	BNT162b2/BNT162b2/BNT162b2/BNT162b2/BA.2	*30	Yes	29	Male
BA.2-23	BNT162b2/BNT162b2/BNT162b2/BA.2	*28	Yes	57	Male
BA.2-24	mRNA-1273/mRNA-1273/BNT162b2/BA.2	*29	Yes	47	Male
BA.2-25	BNT162b2/BNT162b2/BNT162b2/BA.2	*31	Yes	47	Male
BA.2-26	Ad26.COV2.S/mRNA-1273/BA.2	*31	Yes	46	Male
XBB breakthrough (n =19)					
XBB-1	BNT162b2/BNT162b2/BNT162b2/BNT162b2/BNT162b2/XBB	*35	Yes	38	Female
XBB-2	mRNA-1273/mRNA-1273/mRNA-1273/BNT162b2/Moderna bivalent/XBB	*50	Yes	38	Male
XBB-3	BNT162b2/BNT162b2/BNT162b2/Moderna bivalent/XBB	*54	Yes	61	Male
XBB-4	BNT162b2/BNT162b2/mRNA-1273/BNT162b2/XBB	*23	Yes	41	Male
XBB-5	BNT162b2/BNT162b2/BNT162b2/mRNA-1273/XBB	*14	Yes	37	Male
XBB-6	BNT162b2/BNT162b2/mRNA-1273/BNT162b2/XBB	*78	Yes	41	Male
XBB-7	BNT162b2/BNT162b2/BNT162b2/mRNA-1273/XBB	*79	Yes	37	Male
XBB-8	BNT162b2/BNT162b2/BNT162b2/BNT162b2/BNT162b2/XBB	*86	Yes	61	Female
XBB-11	BNT162b2/BNT162b2/BNT162b2/BNT162b2/XBB	*30	Yes	33	Male
XBB-12	BNT162b2/BNT162b2/BNT162b2/BNT162b2/BNT162b2/XBB	*21	Yes	52	Male
XBB-13	BNT162b2/BNT162b2/BNT162b2/XBB	*18	Yes	59	Male
XBB-14	BNT162b2/BNT162b2/BNT162b2/BNT162b2/BNT162b2/XBB	*32	Yes	50	Female
XBB-15	mRNA-1273/mRNA-1273/mRNA-1273/BNT162b2/XBB	*56	Yes	60	Male
XBB-16	mRNA-1273/mRNA-1273/mRNA-1273/mRNA-1273/BNT162b2/XBB	*24	Yes	59	Male
XBB-17	BNT162b2/BNT162b2/BNT162b2/BNT162b2/XBB	*28	Yes	40	Male
XBB-18	Ad26.COV2.S/Ad26.COV2.S/mRNA-1273/BNT162b2/XBB	*29	Yes	46	Female
XBB-19	BNT162b2/BNT162b2/BNT162b2/BNT162b2/BNT162b2/mRNA-1273/XBB	*19	Yes	76	Female
XBB-20	BNT162b2/BNT162b2/mRNA-1273/mRNA-1273/XBB	*28	Yes	61	Female
XBB-21	BNT162b2/BNT162b2/BNT162b2/BNT162b2/XBB	*35	Yes	45	Male

Extended Data Table 1

IC_{50} (μg/mL)	NTD	NTD-SD2	SD1				RBD class 1								RBD class 2				RBD class 3					RBD class 4/1		
	C1520	C1717	S3H3	C68.59	ADARC1	ADARC2	S2K146	BD57-0129	BD56-1302	BD56-1854	Omi-3	Omi-18	BD-515	Omi-42	COV2-2196	XGv347	ZCB11	XGv051	A19-46.1	S309	COV2-2130	LY-COV1404	Beta-54	BD55-4637	SA55	10-40
BA.2	0.001	0.451	0.016	0.046	0.087	0.063	0.039	0.003	0.003	0.001	0.011	0.003	0.012	0.023	0.123	0.001	0.004	0.001	0.045	0.494	0.006	0.001	0.146	0.023	0.010	7.515
XBB.1.5	>10	0.358	0.010	0.054	0.103	0.053	0.104	0.005	0.012	0.007	0.385	2.030	0.157	0.014	>10	>10	>10	0.340	>10	0.343	>10	>10	0.349	0.112	0.018	7.252
EG.5.1	>10	0.779	0.021	0.054	0.162	0.085	0.057	0.003	0.012	0.012	>10	>10	>10	7.459	>10	>10	>10	0.580	>10	0.192	>10	>10	0.329	0.064	0.014	5.397
BA.2.86-V1	0.215	0.693	>10	>10	>10	>10	>10	0.003	0.006	0.002	0.450	0.522	0.115	0.017	>10	>10	>10	>10	>10	9.130	>10	>10	>10	0.019	0.001	1.714
V16_insMPLF	0.003	0.770	0.010	0.035	0.089	0.028	0.056	0.007	0.005	0.003	0.026	0.005	0.015	0.034	0.224	0.003	0.018	0.002	0.025	0.366	0.008	0.001	0.367	0.025	0.015	9.476
BA.2-R21T	0.002	0.350	0.014	0.022	0.084	0.074	0.033	0.004	0.003	0.002	0.020	0.004	0.012	0.031	0.180	0.002	0.016	0.001	0.043	0.430	0.006	0.001	0.267	0.037	0.014	4.374
BA.2-S50L	0.001	0.185	0.018	0.028	0.038	0.099	0.007	0.002	0.002	0.002	0.006	0.002	0.004	0.011	0.103	<0.001	<0.001	<0.001	0.008	0.171	0.003	0.001	0.052	0.010	0.003	1.060
BA.2-H60/V70Δ	0.001	0.505	0.015	0.057	0.073	0.061	0.036	0.004	0.003	0.003	0.013	0.003	0.006	0.027	0.170	0.001	0.008	<0.001	0.033	0.408	0.006	0.001	0.159	0.019	0.009	9.432
BA.2-V127F	0.001	0.499	0.010	0.024	0.062	0.156	0.026	0.005	0.003	0.002	0.015	0.004	0.009	0.027	0.252	0.002	0.008	0.002	0.047	0.457	0.008	<0.001	0.248	0.028	0.012	8.461
BA.2-Y144Δ	0.001	0.362	0.012	0.044	0.066	0.051	0.026	0.007	0.006	0.001	0.020	0.006	0.013	0.029	0.236	0.003	0.012	0.002	0.024	0.408	0.008	0.001	0.221	0.031	0.015	9.400
BA.2-F157S	0.001	0.381	0.010	0.030	0.097	0.051	0.029	0.003	0.003	0.002	0.014	0.004	0.008	0.025	0.119	0.001	0.003	0.001	0.030	0.307	0.004	0.001	0.203	0.018	0.009	6.954
BA.2-R158G	0.001	0.257	0.008	0.030	0.080	0.047	0.033	0.008	0.004	0.002	0.012	0.003	0.006	0.016	0.163	0.001	0.008	<0.001	0.030	0.281	0.007	0.001	0.280	0.017	0.013	6.318
BA.2-N211Δ	0.001	0.171	0.009	0.039	0.093	0.054	0.015	0.003	0.003	0.002	0.014	0.003	0.008	0.030	0.105	0.001	0.004	<0.001	0.030	0.235	0.005	0.001	0.206	0.013	0.009	3.509
BA.2-L212I	0.001	0.486	0.012	0.045	0.069	0.055	0.044	0.004	0.003	0.002	0.015	0.002	0.007	0.022	0.195	0.001	0.007	<0.001	0.043	0.210	0.006	0.001	0.238	0.016	0.013	5.188
BA.2-L216F	0.001	0.696	0.016	0.043	0.109	0.054	0.023	0.003	0.002	0.001	0.012	0.003	0.007	0.020	0.186	0.002	0.009	0.001	0.039	0.388	0.005	0.001	0.181	0.015	0.007	5.708
BA.2-H245N	0.160	0.484	0.013	0.050	0.105	0.160	0.042	0.005	0.004	0.002	0.015	0.004	0.010	0.024	0.185	0.002	0.009	0.002	0.044	0.503	0.008	<0.001	0.241	0.024	0.011	6.877
BA.2-A264D	0.001	0.338	0.012	0.039	0.081	0.052	0.041	0.003	0.003	0.001	0.017	0.004	0.009	0.018	0.161	0.002	0.007	0.001	0.030	0.378	0.008	<0.001	0.236	0.020	0.009	5.380
BA.2-I332V	0.001	0.361	0.017	0.066	0.100	0.217	0.014	0.002	0.001	0.001	0.005	0.002	0.005	0.010	0.100	<0.001	<0.001	0.001	0.016	0.913	0.004	0.001	0.102	0.013	0.004	1.431
BA.2-D339H	0.001	0.739	0.015	0.030	0.061	0.038	0.038	0.006	0.004	0.002	0.018	0.005	0.011	0.024	0.198	0.001	0.010	0.001	0.036	0.108	0.004	0.001	0.426	0.024	0.014	7.557
BA.2-K356T	0.001	0.471	0.006	0.025	0.070	0.030	0.049	0.009	0.005	0.003	0.037	0.005	0.013	0.036	0.370	0.001	0.014	0.001	0.338	>10	0.007	0.001	0.114	0.063	0.025	9.658
BA.2-R403K	0.002	0.172	0.019	0.057	0.087	0.315	0.011	0.002	0.002	0.001	0.004	0.002	0.003	0.008	0.097	<0.001	0.002	<0.001	0.027	0.244	0.005	0.001	0.071	0.006	0.002	1.678
BA.2-V445H	0.001	0.266	0.011	0.023	0.058	0.043	0.029	0.003	0.003	0.001	0.013	0.005	0.009	0.022	0.137	0.002	0.014	0.001	0.042	0.416	0.005	>10	>10	0.037	0.003	7.614
BA.2-G446S	0.001	0.328	0.007	0.032	0.071	0.041	0.016	0.003	0.002	0.001	0.010	0.003	0.008	0.018	0.238	0.001	0.006	0.001	0.065	0.332	0.007	0.001	0.011	0.028	0.006	4.425
BA.2-N450D	0.001	0.742	0.012	0.024	0.084	0.056	0.020	0.004	0.003	0.002	0.013	0.004	0.009	0.022	0.125	0.001	0.007	0.001	0.239	0.316	1.535	0.001	0.113	0.020	0.011	8.862
BA.2-L452W	0.001	0.611	0.015	0.025	0.064	0.068	0.032	0.004	0.003	0.002	0.019	0.003	0.007	0.019	0.191	0.001	0.008	0.002	>10	0.614	0.009	0.001	0.383	0.030	0.012	7.834
BA.2-N460K	0.001	0.414	0.006	0.052	0.113	0.035	0.074	0.009	0.010	0.004	0.378	0.015	0.104	0.071	0.082	<0.001	0.015	0.002	0.063	0.292	0.007	0.001	0.368	0.046	0.015	9.922
BA.2-N481K	0.002	0.448	0.014	0.040	0.066	0.086	0.026	0.005	0.003	0.002	0.015	0.003	0.008	0.022	0.327	0.003	0.011	0.001	0.050	0.301	0.008	0.001	0.206	0.017	0.007	7.480
BA.2-V483Δ	0.002	0.506	0.012	0.029	0.072	0.072	0.032	0.004	0.002	0.002	0.018	0.003	0.009	0.023	0.183	0.003	0.006	0.001	0.072	0.442	0.006	0.001	0.162	0.028	0.012	7.788
BA.2-A484K	0.001	0.424	0.009	0.032	0.064	0.053	0.399	0.005	0.004	0.002	0.015	0.002	0.012	0.033	0.293	0.002	0.006	0.001	0.740	0.404	0.007	0.001	0.119	0.021	0.009	7.142
BA.2-F486P	0.001	0.373	0.010	0.034	0.051	0.050	>10	0.005	0.007	0.005	0.293	0.008	0.017	0.042	>10	>10	>10	0.294	0.036	0.290	0.006	0.001	0.207	0.034	0.010	9.432
BA.2-R493Q	0.003	0.196	0.015	0.056	0.078	0.059	0.003	0.001	0.001	0.001	0.007	0.004	0.003	0.004	0.005	<0.001	<0.001	<0.001	0.020	0.697	0.005	0.001	0.104	0.019	0.005	4.479
BA.2-E554K	0.001	0.428	>10	>10	>10	0.374	0.027	0.004	0.004	0.002	0.013	0.003	0.010	0.015	0.133	0.001	0.007	0.001	0.031	0.289	0.008	<0.001	0.225	0.016	0.010	5.629
BA.2-A570V	0.001	0.192	0.010	0.018	0.052	0.034	0.027	0.004	0.003	0.001	0.012	0.004	0.008	0.016	0.171	0.002	0.006	0.001	0.031	0.337	0.005	<0.001	0.247	0.021	0.009	6.108
BA.2-P621S	0.001	0.410	0.058	0.039	0.112	0.040	0.022	0.003	0.002	0.001	0.013	0.002	0.007	0.012	0.313	0.002	0.006	0.001	0.035	0.234	0.004	<0.001	0.118	0.016	0.013	2.849
BA.2-I670V	0.001	0.303	0.009	0.036	0.049	0.035	0.035	0.005	0.003	0.002	0.015	0.004	0.008	0.021	0.155	0.002	0.007	0.001	0.037	0.327	0.007	0.001	0.234	0.024	0.009	6.229
BA.2-H681R	0.001	0.311	0.008	0.039	0.063	0.040	0.018	0.004	0.003	0.001	0.015	0.004	0.007	0.018	0.137	0.001	0.007	0.001	0.041	0.394	0.007	0.001	0.221	0.023	0.012	8.412
BA.2-S939F	0.001	0.482	0.008	0.019	0.068	0.053	0.016	0.002	0.002	0.001	0.011	0.003	0.005	0.015	0.162	0.001	0.003	0.001	0.019	0.294	0.006	0.001	0.175	0.016	0.008	2.737
BA.2-P1143L	0.001	0.341	0.010	0.026	0.049	0.037	0.014	0.004	0.003	0.001	0.011	0.003	0.005	0.015	0.101	0.001	0.003	0.001	0.021	0.228	0.007	0.001	0.267	0.019	0.010	4.796

>10	<10	<1	<0.1	<0.01

Extended Data Table 2

IC_{50} (μg/mL)	RBD class 1				RBD class 4/1		
	BD56-1302	BD56-1854	Omi-3	Omi-42	BD55-4637	SA55	10-40
BA.2.86-V1	**0.007**	**0.002**	**0.295**	**0.007**	**0.018**	**0.002**	**1.369**
BA.2.86-L50S	0.011	0.003	1.146	0.020	0.037	0.002	2.207
BA.2.86-V332I	0.015	0.003	0.315	0.014	0.044	0.003	5.793
BA.2.86-K403R	0.013	0.004	2.482	0.029	0.080	0.007	3.103
BA.2.86-Q493R	0.011	0.006	>10	0.014	0.036	0.003	0.950

>10	<10	<1	<0.1	<0.01

Extended Data Table 3

nature portfolio

Corresponding author(s): David D. Ho

Last updated by author(s): Sep 28, 2023

Reporting Summary

Nature Portfolio wishes to improve the reproducibility of the work that we publish. This form provides structure for consistency and transparency in reporting. For further information on Nature Portfolio policies, see our Editorial Policies and the Editorial Policy Checklist.

Statistics

For all statistical analyses, confirm that the following items are present in the figure legend, table legend, main text, or Methods section.

n/a	Confirmed	
☐	☒	The exact sample size (*n*) for each experimental group/condition, given as a discrete number and unit of measurement
☐	☒	A statement on whether measurements were taken from distinct samples or whether the same sample was measured repeatedly
☐	☒	The statistical test(s) used AND whether they are one- or two-sided *Only common tests should be described solely by name; describe more complex techniques in the Methods section.*
☒	☐	A description of all covariates tested
☒	☐	A description of any assumptions or corrections, such as tests of normality and adjustment for multiple comparisons
☐	☒	A full description of the statistical parameters including central tendency (e.g. means) or other basic estimates (e.g. regression coefficient) AND variation (e.g. standard deviation) or associated estimates of uncertainty (e.g. confidence intervals)
☐	☒	For null hypothesis testing, the test statistic (e.g. *F*, *t*, *r*) with confidence intervals, effect sizes, degrees of freedom and *P* value noted *Give P values as exact values whenever suitable.*
☒	☐	For Bayesian analysis, information on the choice of priors and Markov chain Monte Carlo settings
☒	☐	For hierarchical and complex designs, identification of the appropriate level for tests and full reporting of outcomes
☒	☐	Estimates of effect sizes (e.g. Cohen's *d*, Pearson's *r*), indicating how they were calculated

Our web collection on statistics for biologists contains articles on many of the points above.

Software and code

Policy information about availability of computer code

Data collection	SoftMax Pro 7.0.2 (Molecular Devices, LLC) was used to measure luminescence in the pseudovirus neutralization assays. Biacore T200 biosensor (Cytiva) was used to measure the spike-ACE2 binding affinity.
Data analysis	GraphPad Prism (version 10.0.2) was used for data visualization and for statistical tests. PISA was used for identifying antibody-spike interface residues. PyMOL v.2.3.2 was used to perform mutagenesis and to generate structural plots. SPR data were fitted with Biacore T200 Evaluation Software (Version 1.0). The Racmacs package (https://acorg.github.io/Racmacs/, version 1.1.4) was used to generate the antigenic cartography.

For manuscripts utilizing custom algorithms or software that are central to the research but not yet described in published literature, software must be made available to editors and reviewers. We strongly encourage code deposition in a community repository (e.g. GitHub). See the Nature Portfolio guidelines for submitting code & software for further information.

Data

Policy information about availability of data

All manuscripts must include a data availability statement. This statement should provide the following information, where applicable:

- Accession codes, unique identifiers, or web links for publicly available datasets
- A description of any restrictions on data availability
- For clinical datasets or third party data, please ensure that the statement adheres to our policy

All experimental data are provided in the manuscript. Materials used in this study will be available under an appropriated Materials Transfer Agreement. Antigenic maps were generated using the Racmacs package (v.1.1.4, https://acorg.github.io/Racmacs/) in R version 4.0.3. SARS-CoV-2 spike sequences were downloaded from the global initiative on sharing all influenza data (GISAID) (https://www.gisaid.org/). The structures used for analysis in this study are available from PDB under IDs 7WKA, 8D8Q, 7MMO, 7TAS, 7TCA, and 7ZF7

Human research participants

Policy information about studies involving human research participants and Sex and Gender in Research.

Reporting on sex and gender	A total of 61 individuals were enrolled in this study. Sex and gender of the participants in this study are described in detail in the Extended Data Table 1: 24 female and 37 male; 22-94 years old.
Population characteristics	A total of 61 individuals were enrolled in this study. Population characteristics for the sera utilized in the pseudovirus neutralization assays are described in the Extended Data Table 1.
Recruitment	Participants volunteered and were enrolled in an observational cohort study at Columbia University Irving Medical Center or in another ongoing cohort at the University of Michigan through the Immunity-Associated with SARS-CoV-2 Study (IASO). Self-selection biases may have affected the demographics of the enrolled population, but are not expected to have impacted the results of this study.
Ethics oversight	All collections were conducted under protocols reviewed and approved by the Institutional Review Board of Columbia University or the Institutional Review Board of the University of Michigan Medical School. All of the participants provided written informed consent.

Note that full information on the approval of the study protocol must also be provided in the manuscript.

Field-specific reporting

Please select the one below that is the best fit for your research. If you are not sure, read the appropriate sections before making your selection.

☒ Life sciences ☐ Behavioural & social sciences ☐ Ecological, evolutionary & environmental sciences

For a reference copy of the document with all sections, see nature.com/documents/nr-reporting-summary-flat.pdf

Life sciences study design

All studies must disclose on these points even when the disclosure is negative.

Sample size	No statistical methods were used to predetermine sample size. We used analogous sample sizes as in previous work (e.g. Wang et al 2021, Nature; Liu et al 2022, Nature; Iketani et al 2022, Nature; Wang et al 2023, Nature), which we had previously determined to be sufficient sample sizes for comparisons between groups for these experiments. The human research participants (n=61) in this study were characterized in 3 cohorts, including “3 shots monovalent + 2 shots bivalent” (n = 17), “BA.2 breakthrough” (n = 25), and “XBB breakthrough” (n = 19) cohorts.
Data exclusions	No data were excluded.
Replication	The hACE2 inhibition assays and pseudovirus neutralization assays were repeated twice independently in technical triplicate with similar results. SPR assays were repeated twice independently with similar results. The results that are shown are representative.
Randomization	As this is an observational study, randomization is not relevant.
Blinding	Virus induced cytopathic effects in the live virus neutralization assays were visually scored for each well in a blinded manner by two independent observers.

Reporting for specific materials, systems and methods

We require information from authors about some types of materials, experimental systems and methods used in many studies. Here, indicate whether each material, system or method listed is relevant to your study. If you are not sure if a list item applies to your research, read the appropriate section before selecting a response.

Materials & experimental systems

n/a	Involved in the study
☐	☒ Antibodies
☐	☒ Eukaryotic cell lines
☒	☐ Palaeontology and archaeology
☒	☐ Animals and other organisms
☒	☐ Clinical data
☒	☐ Dual use research of concern

Methods

n/a	Involved in the study
☒	☐ ChIP-seq
☒	☐ Flow cytometry
☒	☐ MRI-based neuroimaging

Antibodies

Antibodies used

All of the antibodies used in this study were produced in our laboratory. C1520, C1717, S3H3, C68.59, ADARC1, ADARC2, S2K146, BD57-0129, BD56-1302, BD56-1854, Omi-3, Omi-18, BD-515, Omi-42, COV2-2196, XGv347, ZCB11, XGv051, A19-46.1, S309, COV2-2130, LY-COV1404, Beta-54, BD55-4637, SA55, and 10-40 were expressed and purified in-house as described previously in Liu et al 2020, Nature and in the Methods section of this manuscript.

Validation

ADARC1 and ADARC2 that we have been characterizing (our unpublished results) had consistent results on neutralizing BA.2 and XBB.1.5 in our previous assays. The neutralization IC50 value of C68.59 against BA.2 was similar to that has been reported (Guenthoer et al., PNAS 2023). All of the remaining antibodies have been validated in previous studies by neutralization of SARS-CoV-2, e.g. Liu et al 2022, Science Translational Medicine; Wang et al., Nature 2022; Wang et al., Cell 2023; Wang et al., Lancet Infectious Diseases 2023.

Eukaryotic cell lines

Policy information about cell lines and Sex and Gender in Research

Cell line source(s)

HEK293T cells (CRL-3216) for pseudovirus generation and Vero-E6 cells (CRL-1586) for pseudovirus neutralization assays were purchased from the ATCC. Vero-ACE2-TMPRSS2 cells (NR-54970) for authentic virus neutralization assays were obtained from BEI Resources. Expi293 cells (A14527) used for protein expression and purification, were purchased from Thermo Fisher Scientific.

Authentication

Cells were purchased or requested from authenticated vendors and morphology was confirmed visually before use.

Mycoplasma contamination

Cell lines tested mycoplasma negative.

Commonly misidentified lines
(See ICLAC register)

No commonly misidentified cell lines were used in this study.